EXPERIMENTAL PROPAGATION ANALYSIS IN A CDMA 1X MACRO CELL

by

Daryl Meerkerk
Bachelor of Engineering with Distinction
University of Victoria 1999

PROJECT SUBMITTED IN PARTIAL FULFILLMENT OF
THE REQUIREMENTS FOR THE DEGREE OF

MASTER OF ENGINEERING

In the
School
of
Engineering Science

SIMON FRASER UNIVERSITY

Fall 2005

APPROVAL

Name: **Daryl Meerkerk**

Degree: **Master of Engineering**

Title of Project: **Experimental Propagation Analysis in a CDMA 1x Macro Cell**

Examining Committee:

Chair: **Dr. Ash Parameswaran**
Professor of the School of Engineering Science

Dr. Rodney Vaughan
Senior Supervisor
Professor of the School of Engineering Science

Richard LaLau, P.Eng.
External Examiner
UTStarcom Canada

Dr. Nart Bajj
External Examiner
UTStarcom Canada

Date Approved: Nov. 30/2005

SIMON FRASER UNIVERSITY

PARTIAL COPYRIGHT LICENCE

ABSTRACT

Similar to the procedure used for CDMA cell site optimization, a mobile handset was used to collect data regarding the signal quality received from a CDMA base station operating in the 800MHz band. This data was then analyzed to determine its usefulness in defining the radio channel. The study was motivated by the need to gather the data required for optimization of a CDMA 1x cell site with the use of customer handsets rather than with customized test equipment.

Over 50,000 valid measurements were made, which is enough to provide almost complete 2D coverage of the area. Handset location and signal strength were analyzed to recover information regarding mean path loss, fast fading, slow fading, 1D autocorrelation, and 2D autocorrelation. Two and three dimensional plots were produced of these parameters. The results compared favourably with those obtained in previous studies.

ACKNOWLEDGEMENTS

Thank you to Sierra Wireless for provision of mobile station hardware and technical support, to UTStarcom Canada (formerly Telos Technologies) for use of test facilities and infrastructure as well as for support for the measurement campaign, to Rodney and Richard for guidance, and to my wife, Brenda, for enduring.

TABLE OF CONTENTS

LIST OF FIGURES

LIST OF TABLES

LIST OF ABBREVIATIONS AND ACRONYMS

API	Application Program Interface
BSC	Base Station Controller
BSS	Base Station System or Base Station Subsystem
BTS	Base Transceiver Station
Bulkhead	The location of the BTS antenna connectors. The reference point for output power and sensitivity.
CDF	Cumulative Density Function
CDMA	Code Division Multiple Access Cell phone standard initially developed for mobile use and popularized by Qualcomm in the mid 1990s. In some circles CDMA is used for generic CDMA systems; in place of DSS.
CDMA 1x	First generation of CDMA 2000® or single 1.23MHz Channel System The term CDMA 1x is used throughout this paper to identify that a particular version of CDMA is under study and not a generic CDMA or DSS system.
cdma2000®	Standards defined by the 3GPP2 working group TSG-C The term cdma2000® is a registered trademark of the TIA.
dBd	dB gain with reference to a dipole antenna
dBi	dB gain with reference to an isotropic antenna
dBm	dB with reference to 1mW
DSS	Direct Spread Spectrum This is the generic term for many different CDMA technologies. DSS technologies were initially developed by the US military in order to bury transmissions well below the noise floor.
E911	Enhanced 911 This is an FCC initiative to provide public safety officials with accurate location information for a wireless caller.
E_b	Energy per Bit [Joules]
$(E_b/N_o)_{dB}$	Ratio of E_b/N_o expressed in dB. This generally refers to the quality of a received digital signal.
E_C	Energy per Chip [Joules]
$(E_c/I_o)_{dB}$	Ratio of E_c/I_o expressed in dB.

	When referring to a transmit signal this term indicates the power assigned to a particular code channel relative to the total transmit power. When referring to a received signal this term indicates the ratio of the desired code channel to all other signals.
EIRP	Effective Isotropic Radiated Power
	Transmit Power at Bulkhead - Cable Loss + Antenna Gain
Finger	One complete receiver section in a rake receiver.
GOS	Grade of Service
	The GOS is determined primarily by voice quality, dropped call rate and the failed access attempt rate.
GPS	Global Positioning System
gpsOne	A technology introduced by Qualcomm to provide CDMA mobiles with a solution to the E911 initiative. Leverages off of both the GPS system as well as the CDMA protocol to provide position information.
HA	Home Allocation Register
Heliax	Popular low loss cable manufactured by Andrew Corporation
iCell	Brand name of UTStarcom's CDMA BSS
IMG	Intelligent Media Gateway
I_O	Power Spectral Density in Received Channel [Watts/Hz]
	This includes the power of all other users and interferers together with the desired signal. The desired signal typically makes up a small percentage of this power density.
ISM	Industrial, Scientific and Medical Band
	Unlicensed bands.
IS97D	Interim Standard 97D
	Common term for reference [7]: Recommended Minimum Performance Standards for cdma2000 Spread Spectrum Base Stations, 3GPP2 C.S0010-A, 2001.
MSC	Mobile Switching Centre
MSE	Mean Squared Error
N_o	Power Spectral Density of Background Noise [Watts/Hz]
NIC	Network Interface Card
NID	Network Identification
NMEA	Nautical Marine Electronics Association
NOC	Network Operations Centre
Noise Floor	Noise power produced by electron movement
	Approximately -174dBm/Hz at 25 degrees Celsius.
PDF	Probability Density Function

PDSN	Packet Data Switching Node
PN Offset	Offset into the short code which identifies each individual sector.
PRL	Preferred Roaming List
Rake Receiver	A composite baseband receiver which consists of several fingers, each of which contains a complete receiver that tracks multipath components independently.
$(RSSI)_{dBm}$	Received Signal Strength Indication in dBm
RTOS	Real Time Operating System
SDK	Software Development Kit
SID	System Identifier
Soft Handoff	Make before break mobile station handoff
Softer Handoff	Soft Handoff between two sectors of the same BTS
Subs	Subscribers
WiFi	Wireless Fidelity Wireless LAN (WLAN) networks located in ISM bands. Common WiFi standards are 802.11 and 802.16.

1 INTRODUCTION

In this section the motivation for undertaking this study is explained followed by an overview of how the data was gathered and analyzed. At the end of this section a look is taken at what previous researchers have done in this area.

In sections 2 and 3 the process of gathering the measurements is described in detail followed by the process of selecting relevant data out of the measurement database. The mean path loss trend is analyzed and removed in section 4. This leaves slow and fast fading data which is analyzed through the rest of the report. Section 5 introduces the statistical distributions which are commonly found to be useful for propagation analysis. The slow fading properties, fast fading properties, and autocorrelation are analyzed and discussed in sections 6, 7 and 8.

It is expected that the reader has a good understanding of radio technology and signal propagation modelling. A basic reference for propagation modelling can be found in Simon Saunders text [5] or for more detailed work refer to the text by Vaughan and Andersen [13]. Familiarity with CDMA 1x would be an asset but is not assumed. Background for the relevant areas of CDMA will be given in the body of the report. As well, many key terms and acronyms are documented in the 'List of Abbreviations and Acronyms' above.

1.1 Motivation

A good knowledge of the radio environment is important in the development of a radio transmission scheme, for analyzing or optimizing such schemes, and also in the planning of networks using them. In the case of a CDMA system, there are many choices in the planning stage that require an accurate system understanding. As well, after the system has been deployed, there are many optimizations that can be made on the physical layer to improve performance.

This study was motivated by the desire to:

- find what useful data could be collected with a mobile terminal
- determine if this data would be useful in defining the radio channel in which it was operating
- determine if a fingerprint of the radio channel could be useful in CDMA network planning and optimization
- consider how the required data could automatically be gathered by a central location for further analysis

While the jury is still out on many of these considerations, a first step was made in answering them.

Below is a brief overview of CDMA network planning and optimization practices followed by examples of some areas which can benefit from information about the radio channel.

1.1.1 Network Planning of a CDMA System at a Glance

Network Planning is performed before any equipment is deployed. Simulations are performed to determine the correct number and location of the base stations. Good network planning will result in just enough equipment to meet the customer requirements for the given timeframe. In addition, a forward looking plan will also predict the additional equipment required as the user base grows.

In a CDMA system, as in some WiFi architectures, the coverage area of the system is based on the system loading and other parameter choices. When data services are considered the cell sizes are directly related to the data rate required.

Items to consider in CDMA network planning are:

- cell sector coverage areas
- minimizing the handoff region
- supporting the required number of voice calls and data rates

In North America, very good topographical data can be obtained at a reasonable price for most urban or suburban areas. This information can be fed into a planning tool to make good models and consequently good equipment predictions.

Cellular technology is growing rapidly in many developing countries. In these areas topographical information is not as easily available and statistical radio propagation models need to be used.

1.1.2 Optimization of a CDMA System at a Glance

At the optimization stage, the work of the network planners is verified in the field. Adjustments are made to ensure all the desired performance targets are met.

The physical geography is one of the factors which impact the parameters in the initial stages of optimization. This primarily has to do with site locations with respect to each other, to hills, and to other geographical features. Some adjustment parameters related to this are:

- neighbour lists
- antennas tilt and azimuth

Depending on the desired grade of service (GOS) and coverage area the operator can configure many secondary parameters. These parameters determine the GOS and also determine the physical size of the area that BSS can serve. Of course many of them are tradeoffs for each other. For example a system can offer the same GOS over a large area to a few users or over a much smaller area to many users. Voice quality is a key factor in determining the user's perception of the GOS. Some adjustment parameters related to this are:

- forward overhead channel powers
- target FER and target $(E_b/N_o)_{dB}$
- access probe power

The following group of parameters represents a sample of those that need to be set based on the radio environment:

- search window sizes
- handoff thresholds (T_ADD, T_DROP)
- diversity antenna spacing
- finger assignment strategy

The propagation delay from the furthest cell site as well as the dispersion of the signal in the time domain determine the search window size. The expected temporal fade properties of the signal are used to estimate the handoff threshold settings. The minimum required spatial diversity of the receive antennas and the desired finger assignment is also a function of the expected fading characteristics.

1.1.3 Application to Optimization and Algorithm Design

A perfectly optimized system would increase user capacity as well as coverage area for the same equipment costs. Consequently this is an area into which operators are willing to put significant effort. However, in some cases the cost of optimizing a system exceeds the cost of adding more equipment. If an equipment provider could get more out of the available hardware with less effort then profit margins would increase for all involved.

Several of the optimization parameters in the previous section require data, like that provided by this study, to be set knowledgably. For example, the handoff thresholds, antenna spacing, the outer loop power control algorithm, and the search window settings are typically configured to default values since there is very little real data to base them upon. It is believed that a better understanding of the radio environment will help in configuring these items closer to their optimal values.

Consider the search window settings. These need to be set based on the maximum time diversity of a signal. This can be determined by monitoring the finger offsets in the mobile.

The purpose of the outer loop power control algorithm is to determine the target $(E_b/N_o)_{dB}$ set point to achieve the desired FER levels. Vendor specific algorithms are used to iteratively set the $(E_b/N_o)_{dB}$ set point based on long term FER measurements. The correlation between $(E_b/N_o)_{dB}$ and FER is based on the fading environment of the mobile – specifically the user mobility and the terrain type. If fading environments within each cell were known the algorithm could be optimized to provide an appropriate set point more quickly.

The power control bits are sent at a rate of 800 bps. This high rate is used in order to track the path loss into fast Rayleigh fades. If the fading environment and the decorrelation time are known, the power control update rate could be adjusted dynamically in order send the power control bits at the minimum required rate This would reduce overhead data transfer.

For particularly large cells, with over 100km radius, there are fundamental issues with the regular power control schemes. These cells, sometimes called boomer cells, are setup in very rural areas, such as the Australian outback, to cover large sparsely inhabited areas. Since the mobile power is controlled by the BTS, and since the power has to be controlled quickly in order to track fast fading conditions, the round trip delay time has to be small compared to the fading period. Where this is not possible predictive algorithms are used to compensate for the power control loop latency. In order for such algorithms to operate accurately, a good fading model is required.

Consider the hard handoff region and the associated handoff parameters. T_ADD, T_DROP, and several other thresholds and timers specific to the handoff type, control the handoff mechanism. If the radio environment between the mobile and each visible BTS is known, modelling a handoff between the two BTS would allow for selection of the best hand off parameters for that region. Such modelling is not only beneficial to configuration of existing technology but also for the development of future handoff algorithms which make optimal use of macro-diversity channel resources.

The examples above are by no means an exhaustive list. Hopefully they have provided insight into how detailed information about the radio environment, a radio environment fingerprint per se, for each site and ideally for each user, can assist in algorithm development and BTS configuration.

1.2 Eliminating the Drive Tester

1.2.1 Gathering Data with the BSS

Rather than having a team of drive testers using mobile stations to perform drive tests it would be preferred to have the BSS gather the appropriate data itself. The base station can monitor performance indirectly by gathering statistics about access attempts, call completion attempts, and typical throughput rates for both the forward and reverse channels. However the physical layer parameters are a bit more difficult to obtain.

The reverse link path loss and signal quality information can be obtained directly by the BTS. The reverse channel signal strength can be retrieved from the RF front end and the reverse channel FER and $(E_b/N_o)_{dB}$ can be requested from the baseband processing element – typically the CSM5000. Note, however, that if detailed information is collected for each user this can add a huge processing requirement to the RTOS running on the BTS.

With CDMA2000 accurate forward power control was added. Consequently the base station can monitor the forward path by observing the power control bits received from the phone as well its own transmitted power. In order to determine the received level at the mobile, the BTS can request an Outer Loop Report Message (OLRM) which will contain the mobile's current $(E_b/N_o)_{dB}$ target.

In order to learn about interferers and other sectors seen by the mobile, there are several overhead messages which may be utilized. Before a soft handoff is performed the mobile notifies the BTS of observable signal strengths on the same frequency using Pilot Strength Measurement Messages (PSMM) or Power Measurement Report Messages (PMRM). These messages report the pilot power and time offset, as observed by the mobile, for each potential soft handoff candidate. Before a hard handoff is performed the mobile notifies the BTS of signal strengths on a list of frequencies using Candidate Frequency Search Report Messages (CFSRPM). In this case, the mobile will measure the total power, $(RSSI)_{dBm}$, the pilot power, $(E_c/I_o)_{dB}$, and the PN offsets on the requested frequencies as well as on the current serving frequency. There is much information that may be requested from the mobile using these and other messages. The concern, however, is that producing too much unnecessary overhead traffic will reduce the voice quality observed by the user.

As part of the E911 initiative, the US government has mandated that carriers be able to physically locate phone users. For phase I compliance the carrier must report the user's

phone number and the location of the receiving sector. For phase II compliance accuracy of 50 to 300 meters is required in most cases. To obtain this degree of accuracy Qualcomm has developed a feature called gpsOne. This system uses triangulation together with a GPS receiver in the phone. The position determining element is part of the network infrastructure. It collects GPS information from the mobile and also accesses the triangulation information from multiple BTS sectors. The idea is that in rural and suburban environments the phone will be able to acquire a sufficient number of GPS satellites and in a dense urban or indoor environment the phone will be able to see enough BTS sectors to provide accurate location information through triangulation. In both cases the precise timing required by the CDMA network assists in the position determination effort. Support for E911 is required now and has been incorporated into the base band chip sets provided by Qualcomm. The latest chip sets simplify retrieval of this information by allowing it to be obtained without interruption to phone calls in progress. The same position information which is intended for E911 use can be used to tag RF link performance information with the location of the mobile.

By the discussion above, it has been shown that it is possible to obtain very similar information to what was measured in this report using a handset and a GPS receiver, by implementing software on the infrastructure side to automatically request the information from customer mobiles. The analysis performed in this report may be performed with a similar degree of accuracy on the data obtained from the mobiles by the BTS.

It needs to be noted however that although much of the necessary information and messaging is available for channel characterization these messages were not intended for such purposes. Consequently there are some detrimental effects to gathering this data, and data gathering features will need to be enabled selectively or the amount of data collected in a given period of time will need to be limited so that its impact is negligible.

If enough channel characterization data can be obtained, using the methods above, to produce a sufficiently accurate channel fingerprint, or characterization, then drive testers will no longer be required. The system users would be the ones supplying channel performance information using their handsets. The areas the actual users 'test' are naturally much more realistic than the limited drive test paths typically performed by carrier employees. Consequently the collected data will be much more realistic.

1.2.2 Real Time Data Collection and Optimization

Saunders [5] suggests in the closing comments of his text that real time channel predictions will allow a system to optimize itself for the current behaviour of its users and the propagation channel. If propagation data could be continuously collected in real time using spare cycles, adjustments could be made so that the best possible configuration could be used at all times. Typically, large margins are included on most parameters so that the system will be able to handle all possible user behaviours and propagation channels. Adjusting the parameters dynamically would allow an operator to get the most capacity and coverage out of a system at any given time.

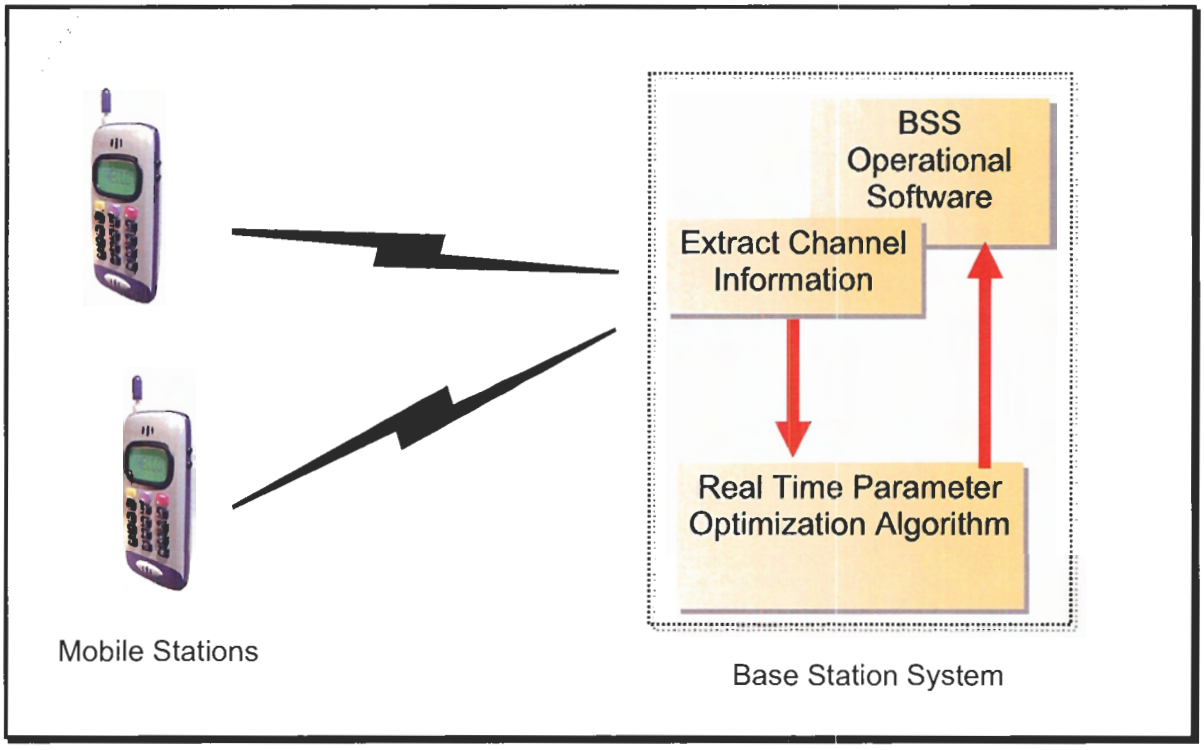

Figure 1 Representation of Real Time Optimization Process

Applying this idea to a CDMA2000 system, the techniques described in the previous section may be used to extract channel information from the BSS and intelligent algorithms could adjust the operational parameters to improve physical layer performance in real time, as shown in figure 1. Many of the BSS parameters which are usually fixed for an entire network could then be optimized on a per site basis.

After deployment a base station could begin optimizing itself for the terrain in which it finds itself. Alternatively, the BSS could be configured to allow for dynamic changes in capacity. For example, during a large civic event, such as a fireworks display, the static capacity models completely break down and many calls are rejected or dropped. In order to rectify this, operators often add extra capacity by reconfiguring neighbour cells to share the load. This situation often repeats itself during unpredictable events such traffic jams. In such cases, it would be desirable for neighbouring BTS sectors to automatically reconfigure themselves to share the load.

1.3 Overview of Work Performed

It is important to note that while the concepts presented in the previous sections motivated this study, bringing these ideas to fruition is a multi-step process. This report only attempts to demonstrate the concept. Implementation is left to base station designers, working with phone vendors, to implement the software features, deploy trial sites, and perform extensive testing.

Showing that the data, which is easily available from a typical mobile phone, is useful in defining the radio environment, with a sufficient degree of detail, is a first step. To that end, a CDMA handset was programmed to lock onto a single isolated macro base station. Signal strength measurements of the CDMA signal along with the position of

each measurement were recorded. The phone together with a handheld GPS receiver provided the same information that could be obtained by customers using gpsOne enabled phones together with the necessary infrastructure enhancements.

Software was written to gather the signal strength from the phone together with its location. The resulting data was analyzed using Matlab to evaluate the mean path loss, shadowing characteristics, fast fading characteristics and the spatial autocorrelation.

The obvious missing parameter for wideband signal analysis is the temporal dispersion. It would have been possible to gather temporal information about the signal by reading the time offset of each finger in the rake receiver. However effort was not put into gathering this information since it is not a parameter that the BTS can obtain from the mobile using currently available messages.

In order to obtain a sufficiently detailed model of the area, it was decided to gather as much data as possible by driving in a 2D grid. This allows for measurement of the 2D path loss and also allows for analysis of the 2D autocorrelation of the slow fading component of the signal.

1.4 Previous Work

Several researchers, including [1]-[5] have gathered data in a linear path by selecting routes of interest through the coverage area. These routes provide representative data from an area. However, in a cellular system, performance information in all areas is of interest.

Mawira [2] documents the procedure used to analyze the autocorrelation and a similar method was used in this report. Mawira comments: "In the near future the dependence of the autocorrelation function with the cartesian separation distance will be studied." That is one of the extensions that will be made with this report.

Many of the researchers who gathered similar data used specialized setups to record the results very accurately. Only Saunders [5] comments briefly on the idea of using customer hardware to provide detailed information about the propagation channel.

It is useful to note, that there are base station vendors, other than UTStarcom, who are actively implementing some of the ideas mentioned above.

2 DATA COLLECTION

2.1 Equipment

2.1.1 Functional Overview

UTStarcom's CDMA 1x base station product, the iCell, was used to broadcast a CDMA signal in the cellular band. This signal was observed by a mobile station, the Sierra Wireless AirCard 555, which was mounted in a vehicle. Figure 2 below gives an overview of the setup. The base station was connected to core network infrastructure including an MSC, IMG, HA and PDSN.

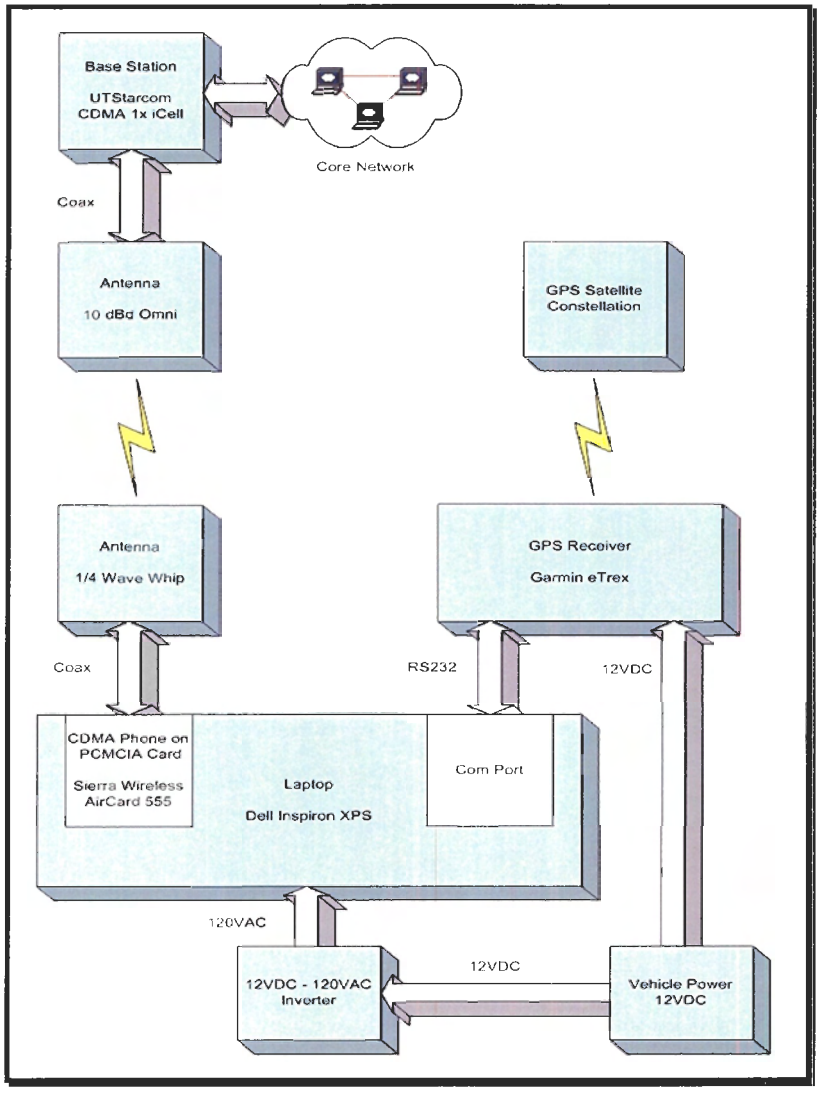

Figure 2 Data Collection Hardware

A single isolated BTS was used with all adjacent BTS operating on different frequencies. The cell was not sectorized and an omni directional antenna was used. This was done to ensure data was collected only from the intended transmitter and to remove the possibility of soft or softer handoffs.

Only the forward path (BTS transmit) was studied. The reverse path will have the same fading conditions although the power level may differ.

2.1.2 Base Station System

In CDMA 1x, up to 128 code channels can exist on the forward path. Each of these code channels occupies the same 1.23MHz bandwidth simultaneously. Of the 128 possible channels, only those indicated in table 1 are of interest. The table is adapted from table 6.5.2-1 in [7].

Code Channel Type	Fraction of Total Power [%]	Fraction of Total Power or $(E_c/I_o)_{dB}$	Absolute Power at the BTS Bulkhead [dBm]
Pilot Channel	20.0	-7.0	23.0
Paging Channel	4.7	-13.3	16.7
Sync Channel	18.8	-7.3	22.7
Traffic Channels	56.5	-2.5	27.5

Table 1 Base Station Transmit Power Distribution

$(E_c/I_o)_{dB}$ refers to the fraction of total power that a particular code channel represents. It is an indication of how deeply the code channel of interest is buried in the composite signal. Due to the processing gain inherent in spread spectrum signals, the $(E_c/I_o)_{dB}$ can be a negative number, and in practice it always is. By definition $(E_c/I_o)_{dB}$ is the ratio of the chip energy for a particular channel (E_C) to the total signal power density (I_O).

While the table indicates the power distribution of a fully loaded cell, in practice the cell rarely operates in this condition. With breathing disabled, the pilot, sync and paging channels remain at static power levels regardless of any traffic on the system. However, the traffic channels are dynamic and in total they can occupy from 0% to 56.5% of the maximum total transmit power.

During testing, the cell site was lightly loaded with only 1 or 2 other test calls being executed. The base station was configured to transmit at a frequency of 884.04 MHz which is also referred to as CDMA channel 468 on band class 0. The transmitter used was a 1 Watt system which means the maximum cumulative power of all the code channels could be up to 30dBm or 1 Watt. The pilot power was configured to be 7dB below the total power and therefore had an absolute level of 23dBm.

The mobile station under test was not making any calls, but rather monitoring the pilot and paging channels. During testing, the pilot channel signal power is recorded and all other channels are ignored.

	Gain [dB]	Pilot Power [dBm]
BSS Bulkhead Connector		23.0
Attenuator	-13.0	
76 meters of 7/8" Heliax at 3.87dB of loss per 100 meters	-2.9	
Pilot Power		7.1
Antenna Gain	12.1	
EIRP		19.2

Table 2 Transmit Power Levels

Table 2 tracks the absolute pilot power through cables losses and antenna gains in the transmitter system. The transmitted signal power in the main beam of the antenna was 19.2dBm.

2.1.3 Transmit Antenna

The transmitting radiator was the SRL480V omni directional antenna from Sinclair. It has 10dBd (12.1 dBi) gain and a 6 degree beamwidth. Sinclair has since replaced the SRL480V with antennas with units of similar performance in the SC480-S series. The antenna gain pattern was obtained from www.sinctech.com and is reproduced below.

When mean path loss trends are analyzed this pattern needs to be compensated for. This is done in section 4.2.

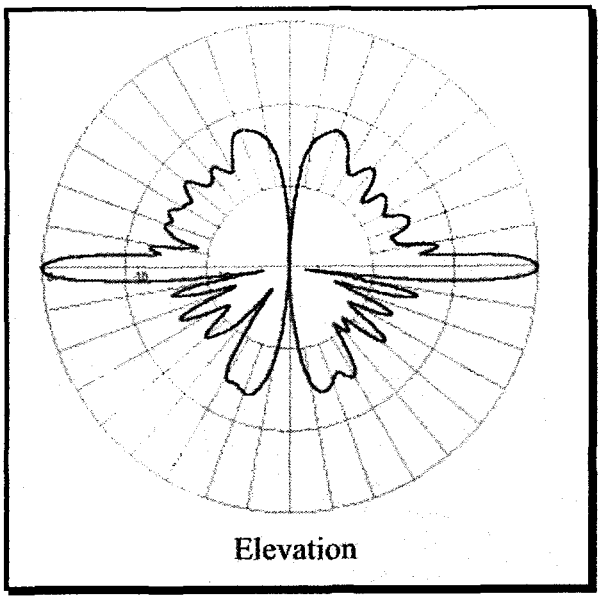

Figure 3 Vertical Pattern of the SRL480V Omni-directional Antenna

The plot in Figure 3 is of the vertical antenna gain – or the gain when antenna is viewed from the side. It is an omni directional antenna and so the horizontal pattern is a uniform circle. Note that the gain scale is marked at 10dB increments with the peak representing the rated gain of 10dBd. The angular scale is marked in 10 degree increments.

2.1.4 Transmitter Site

The transmit antenna was positioned on top of the UTStarcom office building in Richmond, BC. The radiator was located 17 meters above street level, which puts it just slightly above the height of the surrounding buildings. This is a bit lower than typical macro cells in the area, which are closer to 25 meters high. The transmitter site is in the midst of several business parks about 1 km south the Fraser River.

The photograph below shows the main transmit/receive antenna along with the diversity receive antenna. Since only forward path measurements were made, the second antenna, which is only part of the reverse path, does not need to be considered.

Figure 4 Base Station Site with Receive Antenna in the Foreground

2.1.5 Receiver Antenna

The receiving antenna was a ¼ wave magnetic mount whip branded Allgon Kiss. If 100% efficient, this antenna would offer 0dBd (2.1dBi) of gain in the 800MHz band. In addition to the antenna's cable there was an adapter cable – both using RG174 which loss a loss of 0.9dB per meter. Together the cables were approximately 2 meters long. Assuming that it has a reasonably high efficiency (say about 90%) the antenna gain will approximately cover the cable loss and so the receiver is assumed to have a net gain of 0dB.

The antenna was placed in the centre of the roof of the test vehicle. Its height was 2 meters above street level.

For a dipole antenna the antenna gain pattern is not pronounced enough to be of concern when it is a reasonable distance from the transmitter. Since data which is collected too close to the transmitter is discarded in section 3.5, the receiver antenna pattern will not be accounted for.

2.1.6 Mobile Station

The AirCard 555 from Sierra Wireless was chosen for its ability to provide extended signal quality information. The unit is in a PCMCIA form factor but is also a fully

functional phone capable of making voice and data calls. The Aircard is shown in the PCMCIA slot of the laptop in Figure 5.

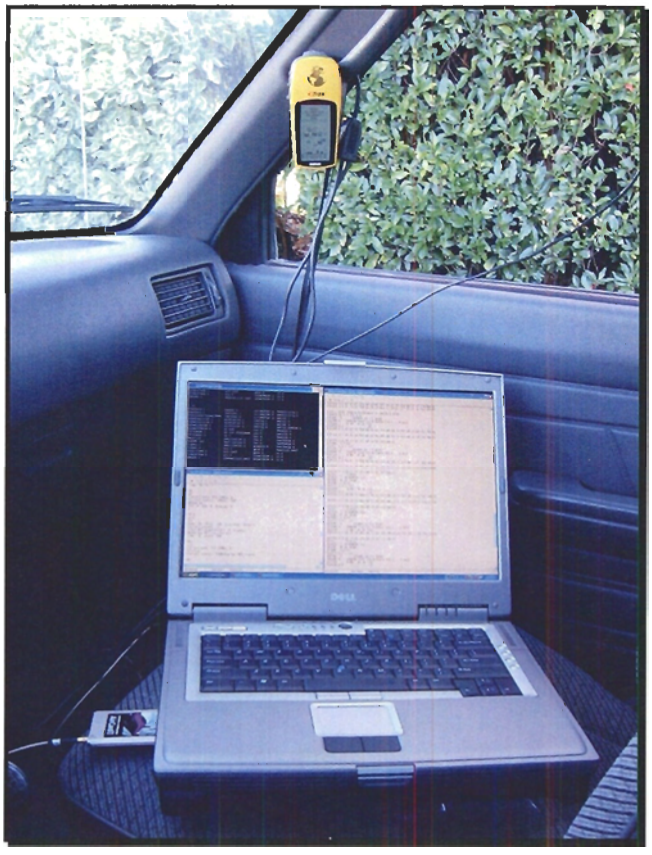

Figure 5 Receiver Equipment

A custom PRL (Preferred Roaming List) was programmed into the AirCard in order to ensure it remained locked to the test cell at all times.

The AirCard appears as both a NIC card and a serial device tc the laptop. A large amount of information is available via a custom API which operates over the network interface. This includes signal quality information from each of the rake receiver's fingers, the active PN set, and the neighbour PN set. The SDK to implement this interface can be requested from Sierra Wireless through their website at www.sierrawireless.com. A smaller amount of information is available via the serial interface which operates by default at 115200 baud. The serial interface uses a custom AT command set to report this information. Only the reduced set of information was required for the purposes of this study and so to simplify programming requirements the latter method was chosen.

The following information was collected from the AirCard:

System Acquisition Status

- Channel
- SID
- NID

- Pilot Acquired Indicator
- Registration Indicator
- Band Class

Signal Quality Information

- $(RSSI)_{dBm}$
- Pilot $(E_c/I_o)_{dB}$

2.1.7 GPS Unit

Position information was provided by the Garmin eTrex GPS unit. This yellow handheld unit is shown at top in figure 5. The eTrex was connected to the laptop via a custom serial cable purchased from Garmin. The unit reported the information indicated below along with other information (which was not of interest) using NMEA formatted data at 4800 baud. This data format is a widely supported but provides rather slow updates.

The following information was collected from the eTrex:

Position Information

- Time
- Northing
- Westing
- Altitude

Position Quality Information

- Position Error Estimate
- Number of Locked Satellites

2.2 Software

Software was developed for the purpose of this study to gather information from the eTrex GPS unit and from the AirCard. The software was written in ANSI C and compiled with gcc on a Cygwin Linux emulator. The Linux compiler was chosen since a previously written code base was available that could be extended for this purpose.

The software runs under the Cygwin environment on a Windows based laptop connected to the eTrex GPS unit and the AirCard. Serial ports to the eTrex and the AirCard are opened simultaneously. Care had to be taken to keep the data reported by the eTrex in sync with the data reported by the AirCard. The simplest solution proved best and a single threaded program was written which polled both interfaces for data.

Position and position quality information is reported every two seconds from the eTrex. While waiting for the next update, the software requests system acquisition information from the AirCard once and requests CDMA signal quality information as many times as it can before an update is received from the eTrex.

In most cases, 10 to 15 sets of CDMA signal information can be collected between each position update. Consequently there is at most 200ms between $(E_c/I_o)_{dB}$ and $(RSSI)_{dBm}$ measurements.

The collected data is written to the console and also stored in comma separated value (CSV) format for easy import into Excel. Refer to the figures below for about 13 seconds of sample data. Figure 6 gives a screen shot of the console and figure 7 shows the resulting data file after import into Excel.

```
meerkerk@Peach ~/common/source/ate
$ ./ap.exe
RESULTS-->> >> AIRPLOTTER <<
RESULTS-->>
Starting AirPlotter...

RESULTS-->> Time, Northing, Westing, Altitude, Error, NumSats, Channel, SID, NID
, Pilot Acquired, Registered, Band/State, RSSI, EcIo, RSSI, EcIo
RESULTS-->>
RESULTS-->> 5252, 4912.7122, 12259.0650,   88.8,   3.2, 4
RESULTS-->> 468, 16422, 0, 1, 1, Cellular CDMA
RESULTS-->> -81, -7, -81, -7, -81, -7, -81, -7, -81, -7, -81, -7,
RESULTS-->>
RESULTS-->> 5254, 4912.7123, 12259.0650,   88.9,   3.2, 4
RESULTS-->> 468, 16422, 0, 1, 1, PCS CDMA
RESULTS-->> -81, -7, -81, -7, -81, -7, -81, -7, -81, -7, -81, -7, -81, -7, -81,
-7, -80, -7, -83, -8, -81, -7, -81, -8, -81, -7, -80, -7,
RESULTS-->>
RESULTS-->> 5256, 4912.7123, 12259.0651,   89.0,   3.5, 4
RESULTS-->> 468, 16422, 0, 1, 1, Cellular CDMA
RESULTS-->> -81, -9, -80, -8, -80, -8, -80, -8, -81, -7, -81, -7, -80, -7, -80,
-8, -80, -7, -80, -8, -80, -8, -79, -8, -79, -8, -80, -8, -79, -8,
RESULTS-->>
RESULTS-->> 5258, 4912.7125, 12259.0652,   89.0,   3.2, 4
RESULTS-->> 468, 16422, 0, 1, 1, Cellular CDMA
RESULTS-->> -79, -9, -79, -9, -79, -8, -80, -9, -80, -8, -80, -8, -79, -8, -80,
-8, -80, -8, -79, -8, -79, -8, -79, -9, -79, -8, -79, -8, -80, -9,
RESULTS-->>
RESULTS-->> 5300, 4912.7126, 12259.0654,   88.9,   3.5, 4
RESULTS-->> 468, 16422, 0, 1, 1, Cellular CDMA
RESULTS-->> -79, -8, -79, -9, -80, -9, -79, -9, -79, -9, -79, -8, -79, -9, -79,
-9, -80, -8, -80, -9, -80, -8, -80, -8, -79, -8, -79, -8, -80, -8,
RESULTS-->>
RESULTS-->> 5302, 4912.7126, 12259.0655,   88.7,   3.2, 4
RESULTS-->> 468, 16422, 0, 1, 1, Cellular CDMA
RESULTS-->> -80, -9, -80, -9, -79, -9, -79, -8, -79, -9, -79, -9, -79, -9, -80,
-8, -80, -8, -79, -8, -79, -9, -79, -9, -79, -9, -79, -9, -79, -9, -79, -8,
RESULTS-->>
RESULTS-->> 5304, 4912.7127, 12259.0657,   88.5,   3.2, 4
RESULTS-->> 468, 16422, 0, 1, 1, Cellular CDMA
```

Figure 6 Output from Data Collection Software

>> AIRPLOTTER <<

Time	Northing	Westing	Altitude	Error	NumSats	Channel	SID	NID	Pilot Acquired	Registered	Band/State
5252	4912.7122	12259.0650	88.8	3.2	4	468	4	1	1	1	Cellular CDMA
5254	4912.7123	12259.0650	88.9	3.2	4	468	4	1	1	1	Cellular CDMA
5256	4912.7123	12259.0651	89.0	3.5	4	468	4	1	1	1	Cellular CDMA
5258	4912.7125	12259.0652	89.0	3.2	4	468	4	1	1	1	Cellular CDMA
5300	4912.7126	12259.0654	88.9	3.5	4	468	4	1	1	1	Cellular CDMA
5302	4912.7126	12259.0655	88.7	3.2	4	468	4	1	1	1	Cellular CDMA
5304	4912.7127	12259.0657	88.5	3.2	4	468	4	1	1	1	Cellular CDMA

RSSI	EcIo	RSSI	EcIo																													
-81	-7	-81	-7	-81	-7	-81	-7	-81	-7	-81	-7																					
-81	-7	-81	-7	-81	-7	-81	-7	-81	-7	-81	-7	-81	-7	-81	-7	-80	-7	-83	-8	-81	-7	-81	-8	-81	-7	-80	-7					
-81	-9	-80	-8	-80	-8	-80	-8	-81	-7	-81	-7	-80	-7	-80	-8	-80	-7	-80	-8	-80	-8	-79	-8	-79	-8	-80	-8	-79	-8			
-79	-9	-79	-9	-79	-8	-80	-9	-80	-8	-80	-8	-79	-8	-80	-8	-80	-8	-79	-8	-79	-8	-79	-9	-79	-8	-79	-8	-80	-9			
-79	-8	-79	-9	-80	-9	-79	-9	-79	-9	-79	-8	-79	-9	-79	-9	-80	-8	-80	-9	-80	-8	-80	-8	-79	-8	-79	-8	-80	-8			
-80	-9	-80	-9	-79	-9	-79	-8	-79	-9	-79	-9	-79	-9	-80	-8	-80	-8	-79	-8	-79	-9	-79	-9	-79	-9	-79	-9	-79	-9	-79	-8	
-79	-8	-79	-9	-80	-8	-80	-9	-79	-9	-79	-9	-79	-9	-79	-8	-79	-9	-79	-9	-79	-9	-79	-9	-80	-8	-80	-8	-79	-8			

Figure 7 Results after CSV File Imported into Excel

In the figure above, the two areas are best read when placed next to each other. Each line of data was recorded every 2 seconds and is referred to as a data set. Each set contains position information as well as 10 or more $(RSSI)_{dBm}$ and $(E_c/I_o)_{dB}$ measurements. The first line of the report records data for a period of less than 2 seconds and so less than 10 RF measurements were made. Such lines were removed from the data set before analysis.

2.3 Measurement Campaign

2.3.1 Area covered

The test vehicle was driven through every publicly accessible road, alleyway, and parking lot in a 2.5km by 4.0km test area shown in figure 8. This provided quite a bit of data, however contrary to the habits of previous researchers [1], [4] the test vehicle never travelled in the same direction for very long. Choosing the area to test was an iterative process. The lock to the BTS was constantly monitored by the driver. When acquisition was lost the test vehicle was driven closer to the base station.

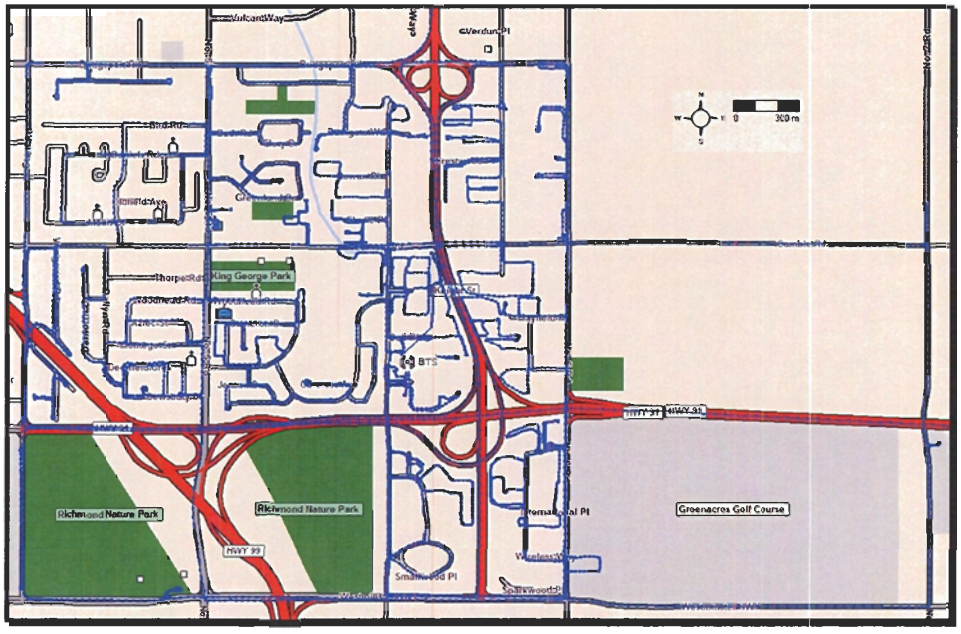

Figure 8 Location of Measured Data Superimposed on Map of Richmond, BC

Note that there are many different land uses in this area. This is evident from this map but can be seen more clearly in satellite picture given in figure 31. Note that the scale in the northeast corner marks a 300m segment.

2.3.2 Test Setup Repeatability

To verify the measurement accuracy of the AirCard and of the GPS receiver the vehicle was held in one spot and data was recorded for 67 minutes. The location used had a view of the horizon that was representative of most measurement locations and the GPS receiver locked onto a typical number of satellites. The intention was to measure the repeatability of the receiver hardware and so the test was done in an area with very few moving objects. The table below shows the repeatability of the key measured parameters.

		Standard Deviation of Measurements	90^{th} Percentile of Measurement Error
GPS	Horizontal Position	1.0 meters	3.3 meters
	Altitude	6.4 meters	8.5 meters
AirCard	$(RSSI)_{dBm}$	1.3 dB	0.8 dB
	$(Ec/Io)_{dB}$	0.8 dB	0.6 dB

Table 3 Standard Deviation of Measured Parameters

Based on the geometry of observed satellites, the GPS unit estimates error for each data point reported. The reported horizontal accuracy was similar to the repeatability shown above. Altitude accuracy however is rated at 15 meters.

For slow fading purposes the repeatability shown above is accurate enough that the receiver could return to the same location a later time and join the data segments together. However, the horizontal position is not repeatable enough to do this when the data will be used for fast fading analysis. If the data is recorded consecutively, though, the relative position accuracy of the GPS over short periods is sufficient.

The absolute accuracy of the receiver in the AirCard was not measured; however it is expected to be within a few dB. Absolute accuracy is only of interest for mean path loss measurements and a few dB is plenty accurate enough for that purpose.

2.3.3 Vehicle Speed

Figure 9 shows the usage pattern of the test vehicle. The bar on the far left is time spent at stoplights, stop signs and the like. The main bump in the middle is the time spent on surface roads and the values on the right represent the time spent on highway travel. The test vehicle represented a typical vehicle usage model for this area. There were no intentional measurements made to simulate pedestrian or in building traffic.

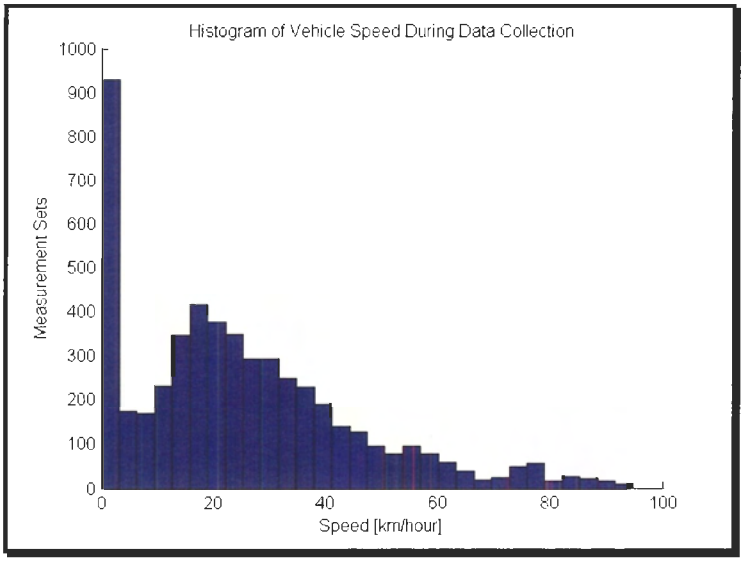

Figure 9 Histogram of the Vehicle Speed During Data Collection

A set of 10 measurements were collected every 2 seconds. Consequently at the fastest speeds of 95 km/hr, or 26.4 meters/second, each measurement was collected every 5.3 meters. However, typically they were much closer together. At speeds of 20 km/hr, or 5.6 m/s, each measurement was collected every 1.1 meters along the drive route.

2.3.4 Data Files

Over a period of two days, 6 sets of data files were recorded. As shown below, a total of 7952 data sets where collected in five files for further analysis and 2000 data sets in a sixth data file were used to verify the repeatability of the data.

Note that with 10 measurements per data set, there were a total of 79,520 measurements. As will be seen in the next section, only about 1/2 to 2/3 of these data sets were useful for further analysis.

File Name	Number of Data Sets	Comments
A.csv	1515	
B.csv	1614	
C.csv	2650	
D.csv	893	
E.csv	1280	
ABCDE.csv	7952	Combination of the above files.
Reference.csv	2000	Vehicle was kept in the same location for 67 minutes.

Table 4 Number of Data Sets in Each File

There were 2 seconds between the collection of each data set. Therefore, the 9952 data sets represents five and half hours of continuous data collection time.

3 SELECTING VALID DATA

From the original data files, data was selected which was deemed not to be extraneous and could generally be relied upon as accurate. The files A.csv through E.csv were combined into one file called ABCDE.csv and processing continued from there.

3.1 Less than Full Data Sets

Due to the way the software was written a variable number of $(E_c/I_o)_{dB}$ and $(RSSI)_{dBm}$ measurements were recorded for each data set. In over 97% of the cases at least 10 pairs of $(E_c/I_o)_{dB}$ and $(RSSI)_{dBm}$ measurements were recorded. The data sets with less than this number were removed from the CSV file. After this process, 7738 data sets remained. This file was renamed ABCDE10.csv and then was imported into Matlab for all remaining analysis.

3.2 No Satellite Lock

The GPS receiver reported the number of satellites acquired for each position reported. The signal is considered valid when the receiver had locked on to three or more satellites. During the testing, six or more satellites were used 95% of the time. In four cases no satellites were acquired while in the remaining cases 4 through 8 satellites were acquired. The four sample sets were removed.

3.3 Pilot Not Acquired

When entering a cellular coverage region the mobile will acquire a pilot signal, register with the base station and then listen for incoming calls on the paging channel. If the mobile is unable to register for a period of time it will enter a sleep mode.

The AirCard provides flags for *Pilot Acquired* and *Registered* conditions and these were monitored during the drive testing. In order to locate the edge of the coverage area the mobile was driven out of coverage in all directions. The data was discarded where the mobile had not acquired the pilot or was unable to register. A total of 2351 data sets were removed which left 5383.

3.4 High Elevation

Almost all of the data was collected in a fairly flat area surrounding the transmission site. In addition, there were a few locations at higher elevations which were unintentionally provided with coverage by the BTS. These included a hill several kilometres outside of the intended coverage area and a bridge over a river adjacent to the coverage area. The 168 data sets collected in these areas were removed by eliminating locations greater than 10 meters above sea level.

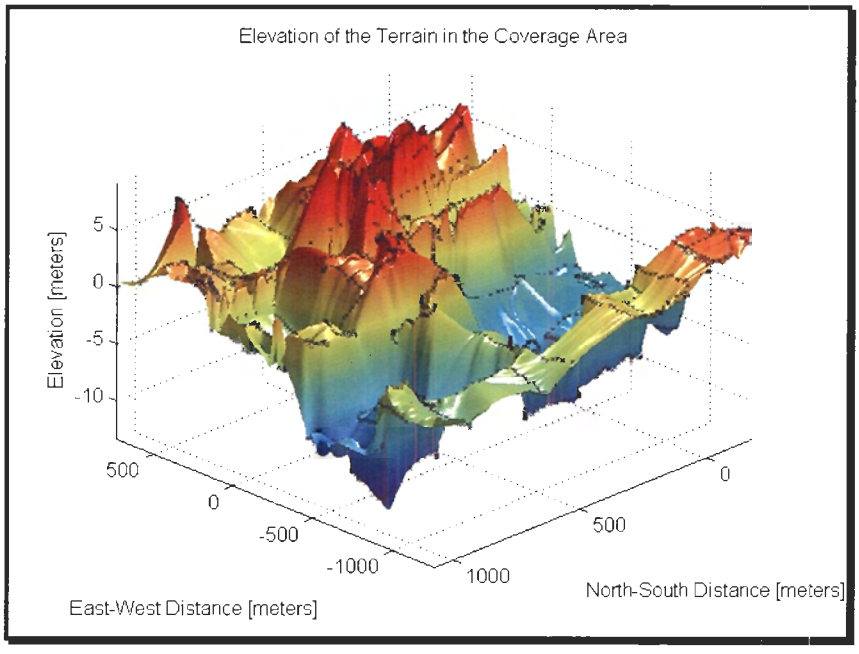

Figure 10 Elevation of the Terrain in the Coverage Area

Figure 10 above shows the elevation of the test vehicle as recorded by the GPS receiver. The measured data points are marked with a black dot while the shaded areas are interpolated from those points. Note also that the vertical axis is highly exaggerated.

In the intended coverage area of the cell site, the terrain is very flat and surface roads within the coverage area are recorded by the GPS receiver to be between -14m below and 10m above sea level. Since the GPS receiver has limited altitude accuracy, see table 3, the data can not be relied on for the precision implied in the plot. In fact elevation data sourced from Geobase shows that the terrain only varies between 1m and 5m above sea level. Due to its flatness, this area provides a good location to study the effects of buildings and other surface clutter without any effects from hills.

3.5 Too Close to BTS

A number of data sets were collected very close to the transmit antenna. There are a number of complications which make it difficult to fit these measurements into a mean path loss trend.

Of greatest difficulty are the side lobes of the BTS antenna. Referring to figure 3, the plot of the transmit antenna gain shows rapidly varying side lobes. The position of the mobile is not known accurately enough to account for these large swings in gain. In addition, the mobile antenna pattern was assumed uniform in section 2.1.5. This no longer holds in close proximity to the BTS. Finally, the vertical distance between the mobile and the BTS is not included in the distance calculations. For work very close to the BTS this distance can not be considered negligible.

While it is acknowledged that the antenna gains form part of the radio channel, they must be accurately accounted for in order to analyze the mean path loss. It is the problem of separating the antenna gain from the path loss that is difficult. To eliminate

such complications, the 148 data sets within 100m of the transmit antenna were removed for all cases except for figure 13. This leaves 5067 data sets for analysis.

3.6 Remaining Data and Analysis Areas

The two cases shown on the left of Table 5 summarize the data filtering described in the sections above. Only figure 13 shows the data collected within 100m of the transmit antenna. All other analysis is performed with these data points removed.

Data Sets	Data Shown in Figure 13	Data Used for 1D Analysis	Data Used for 2D Analysis	Area Shown in 3D Plots
Total Recorded	**7952**	**7952**	**7952**	
Less Than Full Data Sets	214	214	214	
No Satellite Lock	4	4	4	
Pilot Not Acquired	2351	2351	2351	
High Elevation	168	168	168	
Too Close to BTS	0	148	148	
Outside of Selected Area	0	0	899	
Total Used For Analysis	**5215**	**5067**	**4168**	
Total Measurements (10 measurements per data set)	**52150**	**50670**	**41680**	
Area Covered [hectare]	1172	1172	442	249
Measurements per Hectare	44	43	94	>94

Table 5 Summary of Number of Filtered Data Sets

Figure 11 shows the location of the data sets used for 1D analysis. This is a similar area to that shown in figure 8 except that here 2885 data sets have been removed and only 5067 locations remain.

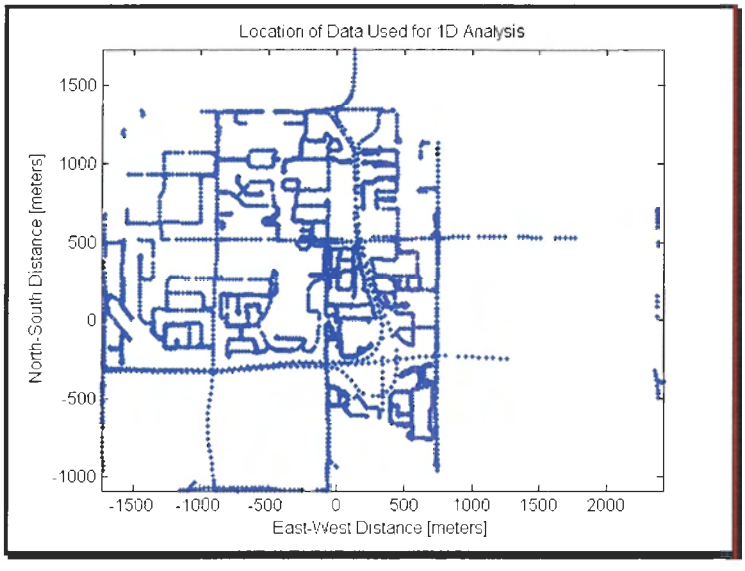

Figure 11 Location of Data Sets Used for 1D Analysis

For 2D analysis, the data needed to be interpolated in order to form a continuous grid of points. To do this well, a smaller region had to be selected where there was sufficient

coverage to make appropriate interpolations. The area used for 2D analysis is shown in figure 12 below. Even with this reduced area the 3D plots showed a few aberrations due to insufficient data. The rectangle shown in the figure indicates a region where the density of data collection was near its highest. The plots were trimmed to show results only in this area. The number of data sets for these cases is shown in the two right most columns of table 5.

Figure 12 Location of Data Sets Used for 2D Analysis

One hectare (10,000m^2) is a commonly used bin size for cellular drive testing analysis which is why it is referenced in table 5. One rule of thumb is that to have a valid measurement, at least 100 frames should be analyzed. Since frames are sent every 20ms this means the data signal should be monitored for 2 seconds. In this report a measurement was taken every 0.2 seconds, so whenever more than 10 measurements are presented per bin (per hectare) this expectation is met. Referring to the bottom row of the table, it can be seen that on average, the number of data points collected easily exceeds this minimum requirement.

If a 100m x 100m grid was laid over figure 12 it would be easy to see that not all bins would contain data. This is very typical for cellular drive testing due to physical limitations. One of the advantages of having the user terminals pass performance information back to the BTS is that many of these empty spaces would get filled in. The empty spaces that do not get filled in would also be informative since coverage is not required in those areas.

4 MEAN PATH LOSS ANALYSIS

A description of the mean path loss trends is presented here. The shadowing and fast fading distributions are covered in sections 6 and 7.

4.1 Received Pilot Power

When received by the mobile, the pilot channel is buried in with traffic channels from the same base station as well as with signals from other base stations and background noise. During the process of extracting the pilot, the power density of the desired signal together with the various interferers is represented by I_O. The $(RSSI)_{dBm}$ is the measurement of the absolute signal strength of the composite signal. The pilot $(E_c/I_o)_{dB}$ measurement represents how deep the pilot signal is buried below the composite signal. Consequently, as given in equation 1, the absolute pilot signal strength is simply the sum of the total signal strength $(RSSI)_{dBm}$ and the pilot $(E_c/I_o)_{dB}$ where the latter is a negative number.

$$RxPilotPower[dBm] = (RSSI)_{dB} + (E_C / I_O)_{dB} \quad (1)$$

The pilot power is used as a reference by all mobiles because it is transmitted at a constant power and is used to define cell boundaries. A plot of received pilot power versus the distance from the radiator is given below.

Note that throughout this section references to pilot power actually refer to an averaged form of the pilot power with the fast fading component removed. The method used to do this is described in section 6.2.

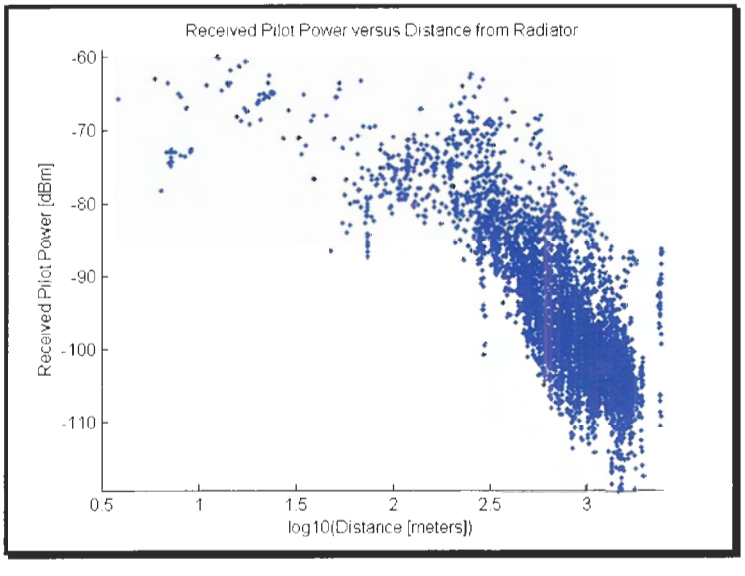

Figure 13 Received Pilot Power versus Distance from Radiator

While the data appears to be without a pattern here, upcoming sections will remove the bias added by the BTS antenna and compare the pilot power to mean path loss trends. By careful examination of figure 13 in comparison with the antenna gain pattern in figure 3 one could surmise how the lobes of the antenna gain correlate with the measured data. While the arcs in the data also bear some resemblance to the two-ray model, all attempts to match the arcs between the data and such a model proved unsuccessful.

A subset of the same data (as discussed in section 3.6) is plotted below in 3D using a linear distance scale. The measured data points are marked with a black dot while the shaded areas are interpolated from those points.

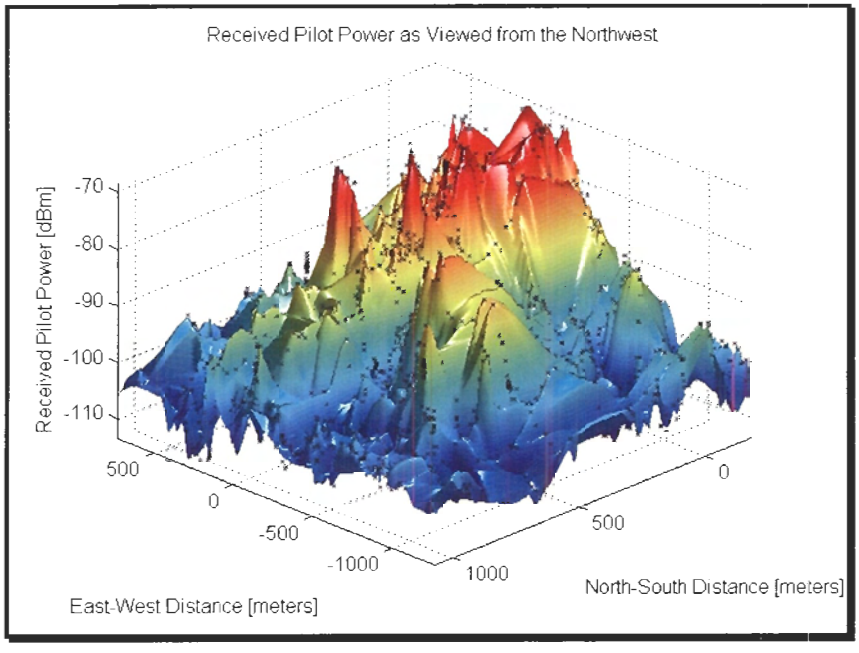

Figure 14 Received Pilot Power as Viewed from the Northwest

One thing to observe from the above plot is that the signal finds a much easier path down roadways than it does over building tops. Refer to figures 8 and 30. There is less than the average path loss directly north of the transmitter. This is because the transmitter provides a strong LOS signal down a main north-south road which is just west of the transmitter. Also, there is a quicker than average drop off of the signal strength west of the transmitter (negative east-west direction). This is due to a long line of condos and a lack of east-west roads for the signal to travel along.

4.2 Correcting for Antenna Gain

Referring to the antenna gain pattern in figure 3, and noting that the transmit antenna is located at a height of 17m while the receive antenna has a height of 2m, it can be calculated that the main lobe will begin to have an impact about 100m away, or at an angle of 8 degrees below horizontal. The transmit antenna gain will continue to increase as the mobile is moved farther from the BTS with its greatest impact occurring at distances greater than 500m.

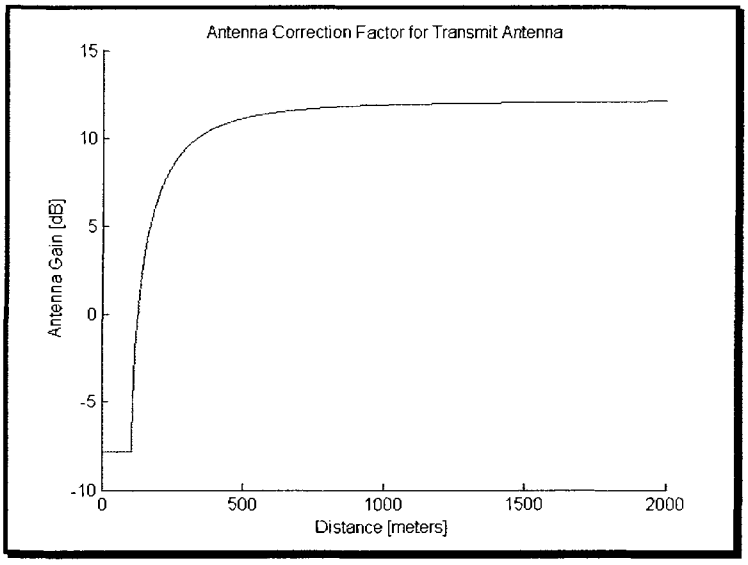

Figure 15 Antenna Correction Factor for Transmit Antenna

For distances greater than 100m from the BTS an antenna gain correction factor was subtracted from the measured data. The resulting data acts as if an isotropic radiator has been used. A plot of the correction factor is shown in figure 15.

As discussed previously the antenna gain below 8 degrees, or closer than 100m from the radiator, changes quite rapidly and would be difficult to compensate for.

4.3 Fitting to Various Models

Equation 2, below, indicates how the antenna gain correction factor was applied.

$$CorrectedPilotPower[dBm] = RxPilotPower - AntennaCorrection \qquad (2)$$

Once the antenna correction factor has been applied and the data below 100m has been removed a trend starts to appear. Figure 16, below, is a plot of the data between 100 meters and 2500 meters with various path loss models superimposed.

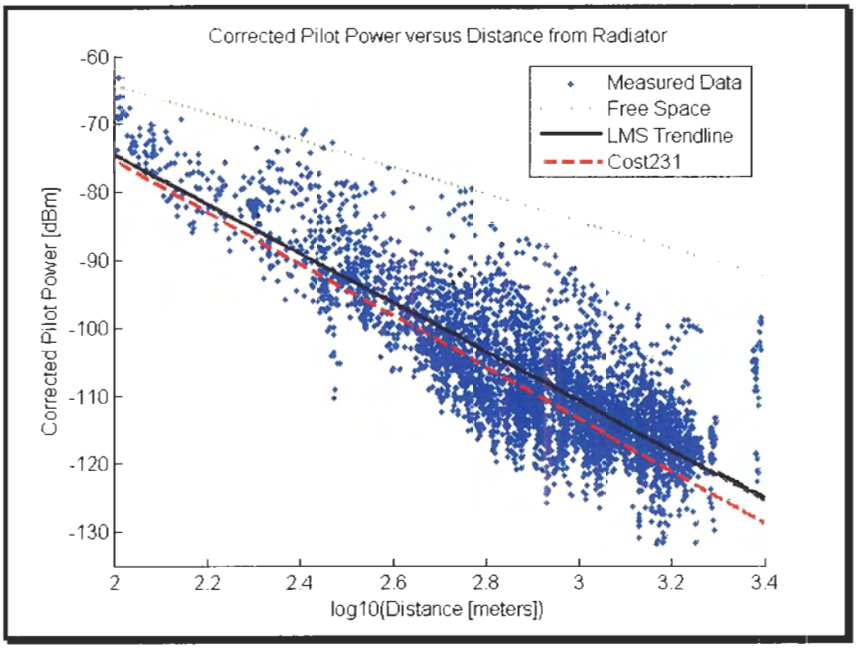

Figure 16 Corrected Pilot Power versus Distance from Radiator

The data at the greatest distance from the radiator, in the above plot, stands out somewhat. This data was collected at the far east of the coverage area in an area used for farming and a golf course. There is less than usual path loss due to a lack of clutter.

4.3.1 LMS Trend Line

For a given frequency, antenna height and terrain type, most path loss models used for macro cells may be simplified to the form given in equation 3. In this study the radius, *r*, has units of meters and the equivalent path loss at 1m, PL_0 is in dB. The parameter, *n*, is referred to the path loss exponent and is independent of the selected units for *r*.

$$PL\_Trend[dB] = PL_0 + 10n\log_{10} r \qquad (3)$$

To produce a trend line for figure 16, a least means squared fit to equation 3 was applied to the corrected pilot power data. The trend line is an estimate of the corrected pilot power and can be represented by equation 4.

$$CorrectedPilotPowerEstimate[dB] = TxPilotPower - PL\_Trend - AntennaCorrection \qquad (4)$$

As given in Table 2 the value of *(TxPilotPower – AntennaCorrection)* is 7.1dBm. The LMS fit found the path loss exponent, *n*, to be 3.61. Using these values equation 4 was plotted in figure 16 as the solid black line marked LMS trendline.

Several previous studies have also found a path loss exponent of close to 4 when measurements or analysis has been performed on macro cells. Table 6 below is adapted from table 8.3 in Saunders [5].

Researcher	Path Loss Exponent, *n*
Egli, [17]	4
Lee (suburban), [18], [19]	3.84
Ibrahim, [20]	4
Allesbrook, [21]	4
Walfisch – Bertoni, [22]	3.8
Walfisch-Ikegami (Cost 231), [12]	3.8
This study	**3.61**

Table 6 Path Loss Exponents Observed by Other Researchers

4.3.2 Friis Free Space Model

The Friis free space model is derived by analyzing transmission from an ideal isotropic radiator. As the signal disperses in three dimensions the signal strength at any given point decreases with the square of the distance from the radiator.

The model is given by equation 5 where the radius, *r*, is in km and the frequency, *f*, is in MHz.

$$PL\_Friis[dB] = 32.45 + 20\log10(r) + 20\log10(f) \quad (5)$$

Since this is an idealized model, with no consideration for obstructions, it represents the least possible loss between two points. Of course in an area of constructive interference slightly less path loss may be observed. Generally however, this model is not very useful when analyzing mobile radio propagation since it drastically underestimates the path loss.

Referring to figure 16, the Friis model, plotted as the dotted green line, correlates well with the signals with the lowest path loss. In these areas there is likely a line a sight path between the transmitter and the mobile station.

4.3.3 Cost231 Model

The Cost231 model [12] is an integrated model which relies on the work of Walfisch, Ikegami, Bertoni [22] and others. It is based on a three part theoretical model which has been well tested with various measurement campaigns. The first part is the free space loss, *PL_Friis*. The second part, L_{msd}, is the path loss caused by the signal passing over multiple rooftops and is modelled by multiple knife edge diffraction. The last part, L_{sd}, is caused by the diffraction and scattering from the last building down to the street and is modelled mainly by single knife edge diffraction. These components are shown in equation 6. For a more detail description refer to [12].

$$PL\_Cost231[dB] = PL\_Friis + L_{msd} + L_{sd} \quad (6)$$

The Cost231 model has many parameters which are fairly easy to fix in a homogeneous environment. However, the land use in the measurement area varies from farming to industrial to condominiums. Consequently, fitting the COST231 model to this area proved difficult.

Plotted as the dashed red line in figure 16, the Cost231 model, using the parameters selected below, shows quite a reasonable fit to the data.

Base Station Height (hb): Measured at 16.7 meters.

Mobile Station Height (hm): Measured at 2.0 meters.

Typical Building Height (h0): With reference to Richmond bylaws [10], industrial buildings are rated at a maximum of 12 meters and residential buildings are rated at a maximum height of between 9 and 10 meters high. Since the area is fairly evenly split between the two types of buildings, on average this would be 10.75 meters for the maximum height. The area has been built up fairly recently and so most buildings are expected to be at their maximum height. A value of 10.75 meters was used.

Spacing between Buildings (w): Using Google Earth (see earth.google.com) building spacing was measured through the measurement region. In residential and industrial areas the distance between buildings was observed to be 30 to 70 meters. However in the areas used for parks, schools, farming, green areas, or highways a spacing of 200 to 400 meters was observed. Since about $7/8^{th}$ of the area is industrial or residential, a weighted average value of 80 meters was used.

Distance from Last Building (wm): The recommended value for rough work is w/2. This assumes that the vehicle is driven close to the middle of the road or midway between two buildings.

Street Orientation (ϕ): The recommended value for rough work is 90 degrees.

5 EXPECTED STATISTICAL DISTRIBUTIONS

In sections 6 and 7 the slow fading and the fast fading components of the signal will be studied. Log-normal fading and Rayleigh fading are typically observed in these cases. The appropriate distributions are presented here for reference.

5.1 Normal and Log-Normal

The PDF of a zero-mean normal distribution is given in equation 7. The standard deviation is given by σ.

$$p(x) = \frac{1}{\sqrt{2\pi}\sigma} e^{\frac{-x^2}{2\sigma^2}} \tag{7}$$

From the central limit theorem it is known that when multiple random actions combine additively the resulting distribution tends towards normal and when they combine multiplicatively they tend towards log-normal [16]. The slow fading distribution is made up of the means of the fast fading distribution. These means, which vary over time due to large scale shadowing and other perturbations to the system, tend to have a log-normal distribution [5].

In this study the power is being observed in terms of dB and so the free variable in equation 7 is in terms of dB. Consequently if the distribution in decibels appears to be normally distributed the signal will actually have a log-normal distribution.

For reference, the histogram and CDF of 10,000 normally distributed random data points are plotted below in figure 17. The distribution has zero mean and a standard deviation of one. On the right the CDF of the normal distribution is plotted on normal distribution paper. The CDF is distorted so that if it had a perfectly normal distribution it would generate a straight line. The dashed red line represents such an ideal distribution.

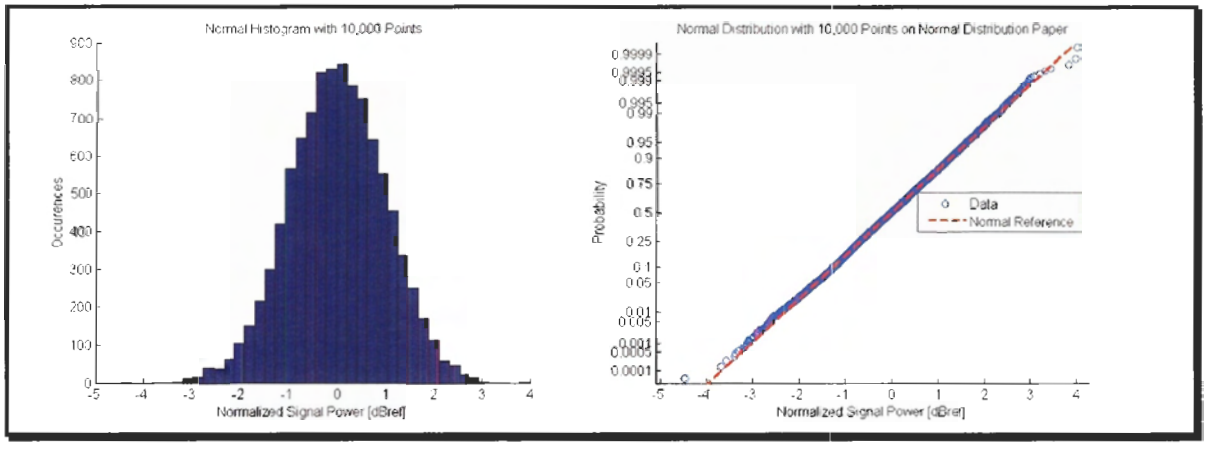

Figure 17 Reference Normal Distribution

On normal probability paper, the tails of the normally distributed data, plotted as circles, will obviously align very well with the reference. With 10,000 data points plotted it can be seen that the tails start to diverge a little when probabilities of about 5 in 10,000 are observed.

5.2 Rayleigh and Exponential

The PDF of the Rayleigh distribution with a parameter, *b*, is given in equation 8.

$$p(x) = \frac{x}{b^2} e^{\frac{-x^2}{2b^2}} \tag{8}$$

Fast fading components, where two or more paths are adding constructively and then destructively over distances in the order of a wavelength tend to follow a Rayleigh distribution.

For reference, the histogram and CDF of 10,000 Rayleigh distributed random data points are plotted below in figure 18. The distribution has a parameter, *b*, of 5. On the right the CDF of the Rayleigh distribution is plotted on normal distribution paper. A normal distribution would generate a straight line. Note the characteristic divergence of the lower tail from the normal reference. With 10,000 data points plotted it can be seen that the tails start to diverge when probabilities of about 500 in 10,000 are observed.

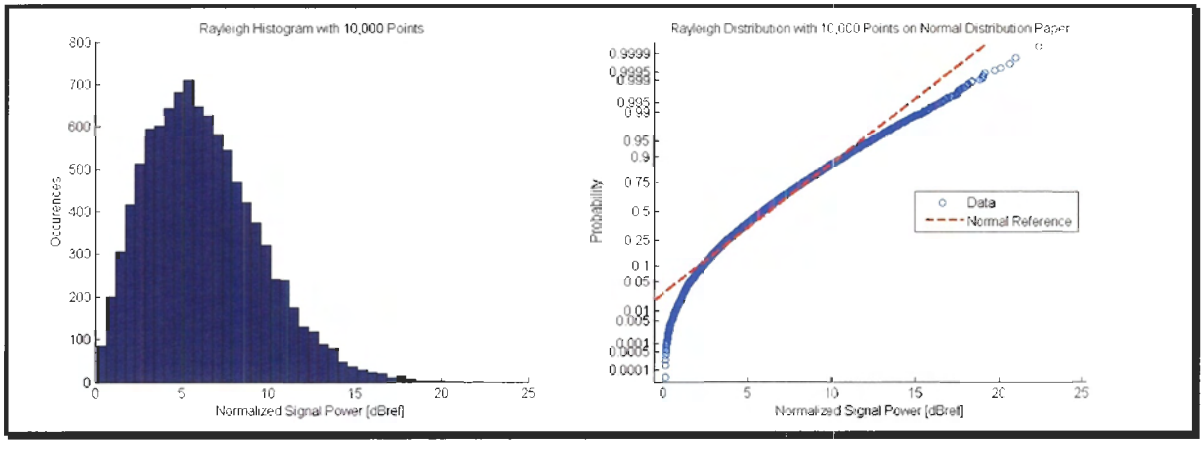

Figure 18 Reference Rayleigh Distribution

It is important to note that it is the linear electric field strength that tends to follow the Rayleigh distribution and not the power reported in dBm. When the field strength has a Rayleigh distribution the power in dB will have an exponential distribution [11]. Similarly, if the distribution in decibels appears to be exponentially distributed the signal will be experiencing Rayleigh fading.

The PDF of an exponential distribution with a mean, μ, is given in equation 9.

$$p(x) = \frac{1}{2\mu^2} e^{\frac{-x}{2\mu^2}} \tag{9}$$

For reference, the histogram and CDF of 10,000 exponentially distributed random data points are plotted below in figure 19. The distribution has a mean, μ, of 5. On the right the CDF of the exponential distribution is plotted on normal distribution paper. Note the severe divergence of both tails from the normal reference.

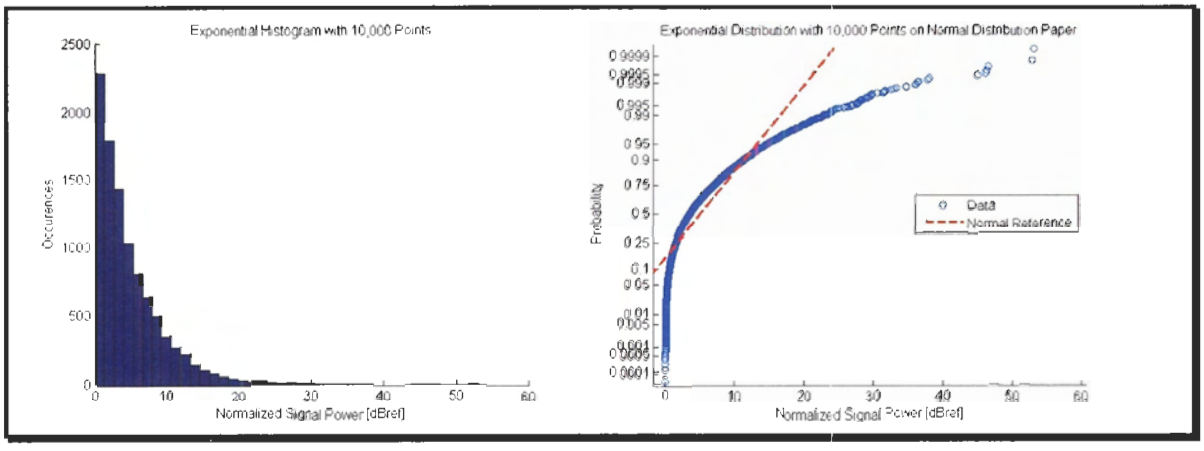

Figure 19 Reference Exponential Distribution

5.3 Combinations and Derivatives the of Normal and Rayleigh Distributions

The following distributions represent various ways of combining the normal and Rayleigh distributions.

The Ricean distribution is commonly seen in narrowband fast fading signals when there are both direct and indirect paths to the transmitter present. The fading will vary from a Rayleigh distribution to a Ricean distribution depending on the ratio of the direct LOS signal to the multi-path NLOS components. A complete NLOS signal would be Rayleigh and as the strength of the LOS component rose the distribution would become more normal. A Rice factor is attributed to the distribution to identify to what degree it emulates the Rayleigh or the normal distribution.

The Suzuki distribution is seen when both the normal slow fading and Rayleigh fast fading are combined in the same signal. The Rayleigh fading signal has local means which have a log-normal distribution. To simplify matters, when at all possible, the fast and slow fading components are separated before analysis and so that this distribution is not required.

The Weibull distribution and the Nakagami m distributions are generalizations of the Rayleigh distribution. They remove some of the assumptions that the Rayleigh distribution makes. Consequently, by adjusting parameters, these distributions can both be reduced to the Rayleigh distribution.

For further information on these and other relevant distributions refer to chapter 6 in Griffiths [11], Appendix C in Vaughan and Andersen [13] or chapter 2.5 in Bajj [16].

6 SLOW FADING ANALYSIS

A radiated signal undergoes path loss due to dispersion and distance from the transmitter, it undergoes slow fades caused by obstacles between the transmitter and the receiver, and it undergoes fast fading caused by multiple signal paths arriving at the receiver. Section 4 studied the mean path loss. In this section, the slow fades will be isolated and studied further.

To isolate the slow fading component of the signal, the mean path needs to be subtracted and averaging needs to be performed to remove the fast fading component.

6.1 Removing Mean Path Loss

Equations 2 and 4 show how the *Corrected Pilot Power* and the *Corrected Pilot Power Estimate* are obtained. The difference between the measured data and the mean path loss estimate is the fading component.

$$CompositeFadingComponent[dB] = CorrectedPilotPower - CorrectedPilotPowerEstimate \quad (10)$$

The composite fading component defined in equation 10 contains both the fast fading and the slow fading components.

6.2 Selection of the Slow Fading Component

Methods for separating the fast fading and slow fading components are well documented.

Mawira [2] uses averages of 10 meters to produce local means for 154MHz, 461MHz, and 922MHz signals.

Lee [15] shows that local means from data intervals 20-40 wavelengths long will provide good estimates of local average power. For an 884MHz signal this corresponds to 7 to 14 meters.

M. LeCours et al. [4] filter the data with a cutoff frequency of 0.125 cycles per wavelength with a stopband starting at 0.1875 cycles per wavelength. This has a similar effect to performing a sliding weighted average over 5.3 to 12 wavelengths. At the frequency of interest this corresponds to a distance of 1.8 to 4 meters.

Gudmundson [1] uses 27m averaging in suburban areas.

The speed of the test vehicle is displayed figure 9. On average, the speed was 7 m/s and 10 data points were taken every 2 seconds. The manner in which the data was recorded lends itself to averaging of the 10 data points which are tagged with a single position. Note that although they are tagged with the same position, the 10 data points are measured between that position and the next recorded position.

Consequently, the 10 data points, taken on average 1.4 meters apart, were averaged and recorded with their position. This produced, on average, 14 meter local means. This

is consistent with the procedures of Mawira, Gudmundson and Lee mentioned above. The vehicle was also driven on the highway at about 25m/s during a brief spell. In this worst case scenario the local means were produced over a 50m distance.

Finally to provide a smooth transition between the local means a spline interpolation was applied. The resulting signals are shown in figures 20 and 21 below.

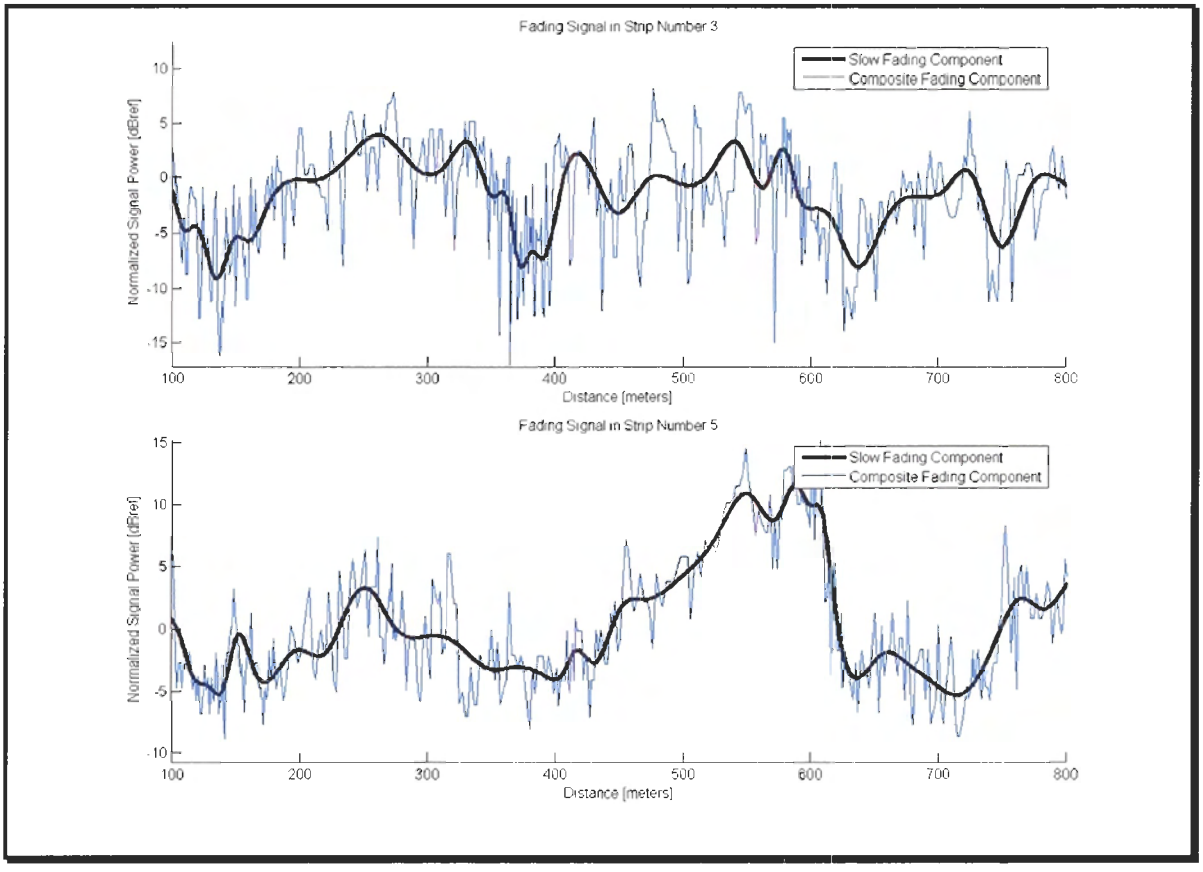

Figure 20 Fading Signal in Selected Strips from Residential Area

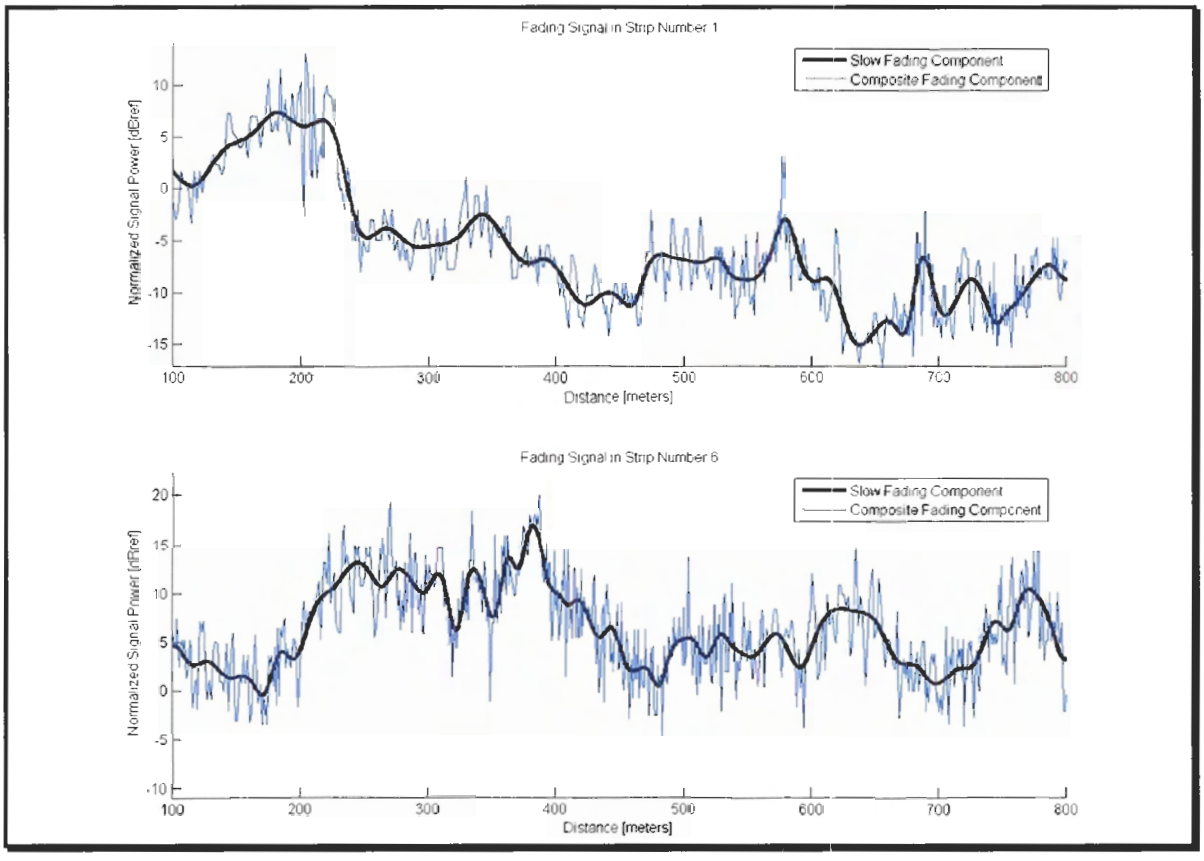

Figure 21 Fading Signal in Selected Strips from an Industrial Area

The distance along the bottom is an indication of the distance the test vehicle travelled - which is not necessarily in a straight line.

These are the strips of data that will be used to determine the 1D autocorrelation. The criteria for their selection are described in section 8.1.2 and their location is shown in figure 31.

Represented functionally the process of separating the slow fading component can be shown as in Equation 11.

$$SlowFadingComponent[dB] = SplineSmoothing(LocalMeans(CompositeFadingComponent)) \quad (11)$$

The slow fading component, in a subset of the measurement region, is plotted below in 3D using a linear distance scale.

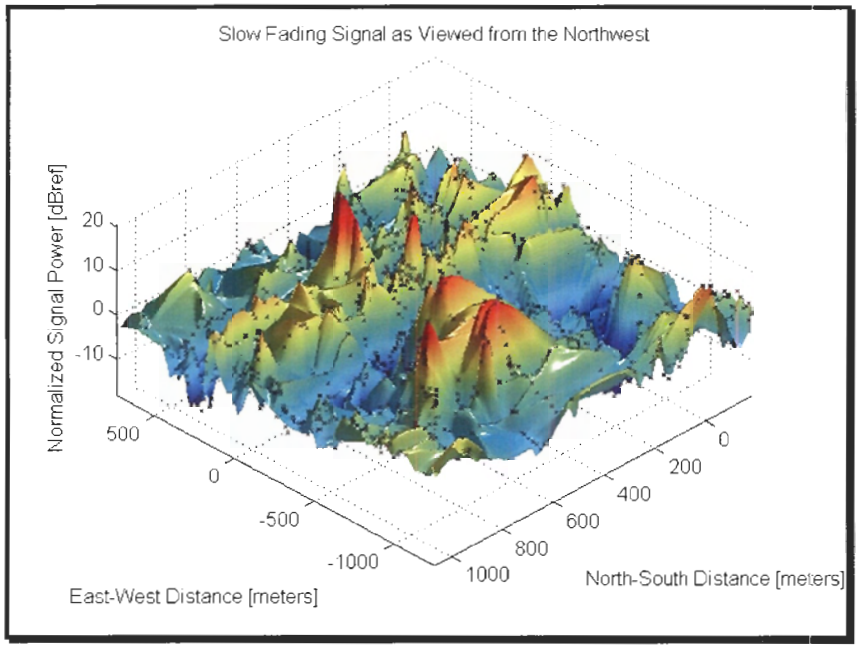

Figure 22 Slow Fading Signal as Viewed from the Northwest

This is the data that will be used to determine the 2D autocorrelation. The measured data points are marked with a black dot while the shaded areas are interpolated from those points.

6.3 Statistical Distribution of the Slow Fading Component

The histogram and CDF of the composite fading signal are plotted below in figure 23. Compare this distribution to the reference distributions provided in figures 17, 18 and 19. With 50,670 data points plotted it can be seen that the tails diverge only slightly when probabilities of about 5 in 50,000 are observed.

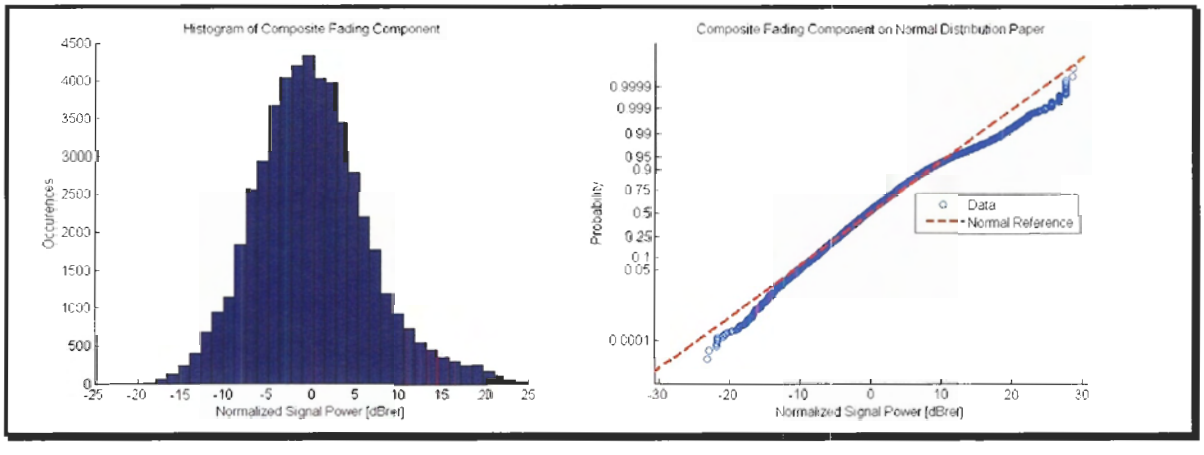

Figure 23 Probability Distribution of All Data

The composite fading signal has zero mean and a standard deviation of 6.6dB. By comparison with the reference distributions, the composite fading signal is similar to a log-normal distribution. If there was heavy underlying Rayleigh fading the composite

fading signal would be expected to have more of a Suzuki distribution. However this does not appear to be the case. Analysis of the fast fading component in section 7 sheds more light on this.

The histogram and CDF of the slow fading signal are plotted below in figure 24. Compare this distribution to the reference distributions provided in figures 17, 18 and 19. With 5067 data points plotted it can be seen that the lower tail diverges slightly when probabilities of about 5 in 5,000 are observed. The upper tail starts to stray slightly when probabilities of about 50 - 100 in 5000 are observed.

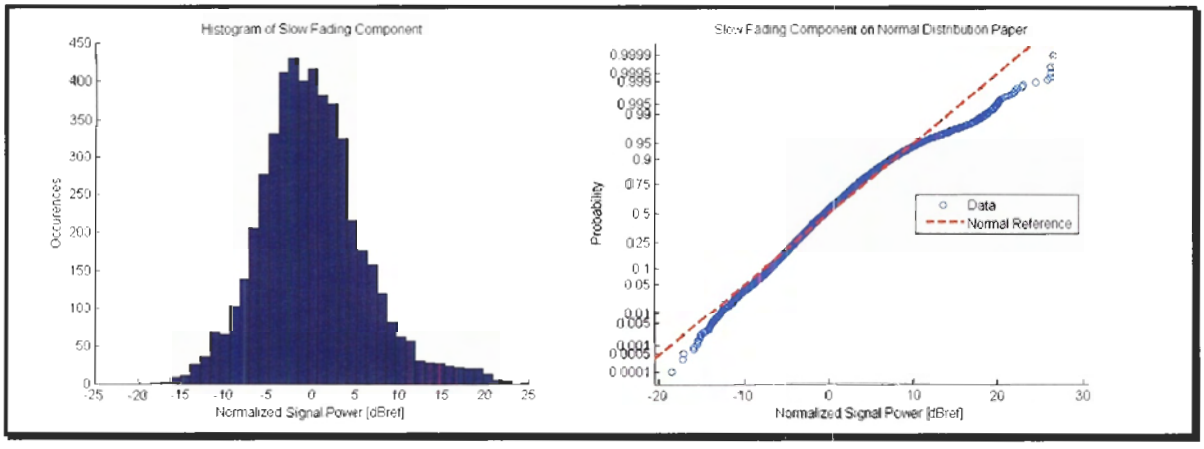

Figure 24 Probability Distribution of Shadowing Data

The slow fading signal has zero mean and a standard deviation of 6.0dB. By comparison with the reference distributions, the slow fading signal is similar to a log-normal distribution.

6.4 Location Variability

Location variability is the variance observed on a distribution of the slow fading signal. In general the variance at a given distance is caused by buildings, foliage, moving objects and hills. Table 7, below, is a list of location variability results observed by other researchers. Some of the values were taken from compilations made by Jakes [14] and Saunders [5].

Researcher	Standard Deviation of Composite Fading Component [dB]	Standard Deviation of Slow Fading Component [dB]	Frequency Measured [MHz]
Algans, Pedersen and Mogensen [3]		6.1 (suburban) 7.3 – 8.5 (typical urban)	1800
LeCours, et al [4]	4.231 (suburban) 4.781 (low density urban)	2.648 (suburban) 3.275 (low density urban)	900
Black [6]		5.8 – 9	850
Okumura [8]		6.9 (urban) 8.1 (suburban, hills)	800
Ibrahim [20]		6.4	900
Egli [17]		11.7	500
This Study	**6.6**	**6.0**	**884**

Table 7 Location Variability Observed by Other Researchers

The measured slow fading standard deviation of 6.0dB compared quite favourably with those observed by previous researchers. The fact that there were no hills in the measurement area likely caused the measured standard deviation to be on the low side.

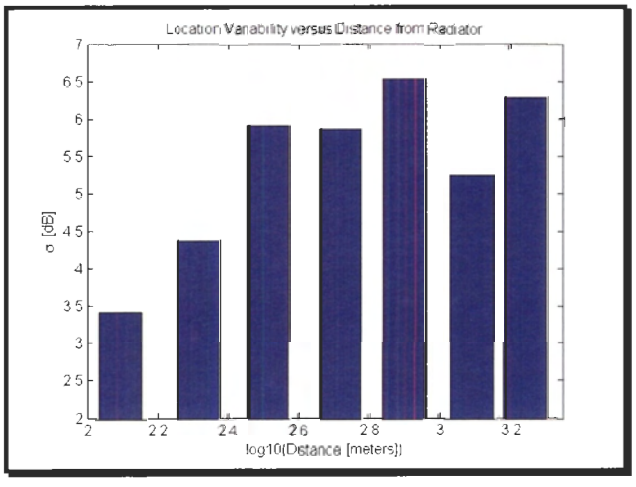

Figure 25 Location Variability versus Distance from Radiator

In the figure above, the data was broken into 7 bins based on distance from the transmitter. It can be seen that sigma increases with distance from the radiator and then levels off. This is simply due to the fact that, at larger distances there are more random obstacles affecting the signal. Consequently the variance increases.

7 FAST FADING ANALYSIS

7.1 CDMA 1x as a Wideband Signal

A signal is typically considered wideband when the delay spread is significantly wider than the chip time. The parameter typically used to define the delay spread is τ_{RMS}, the RMS delay spread. Calculated as shown in equation 12, τ_{RMS}, gives an indication of the time spread of the identifiable paths.

$$\tau_{RMS} = \sqrt{\frac{1}{P_T}\sum_{i=1}^{n} P_i \tau_i^2 - \tau_0^2} \qquad (12)$$

Shown in figure 26 is a signal with six received paths. τ_0 is the mean excess delay, P_T is the total power, P_i is the power of the i^{th} path and τ_i is the time offset of the i^{th} path.

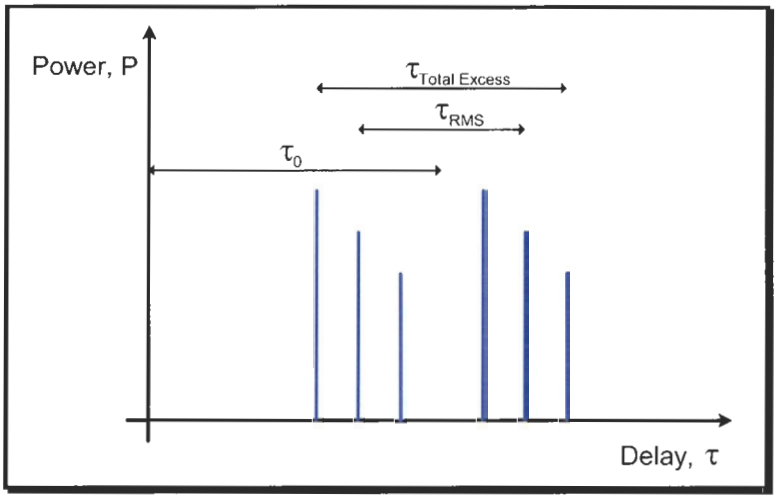

Figure 26 Delay Spread Parameters

Due to the reduced number of scatterers in a rural environment the RMS delay spread tends to be less than that in a dense urban environment. However, this is not necessarily true of the total excess delay, $\tau_{Total\ Excess}$. The total excess delay is the time from the first signal arrival to the last echo. In rural environments a weak signal could arrive from a far off reflector. Since this weak reflection has little impact on receiver performance, the RMS delay spread gives a better picture of the usable received paths.

Although the delay spread was not recorded in this measurement campaign, several other researchers have well documented results.

Algans, Pedersen and Mogensen, [3] found delay spreads in a suburban environment to be greater than 1μs five percent of the time and in a typical urban environment they found that the delay spread was greater than 1μs forty percent of the time. Saunders [5]

records typical delay spreads of <1 μs in a suburban macro cell and 1-3μs in an urban macro cell.

The chip rate in the system under test was 1.2288 MHz which translates to a chip time of 0.814 μs. The measurement area has a mix of land use types but can predominantly be classified as suburban. Since the chip rate is close the expected delay spread it is expected that the signal will demonstrate both narrowband and wideband characteristics depending on the location of the mobile.

7.2 Frequency Selective Fading

When experiencing time delays greater than about 1μs, one of the wideband effects that a CDMA 1x signal will experience is frequency selective fading.

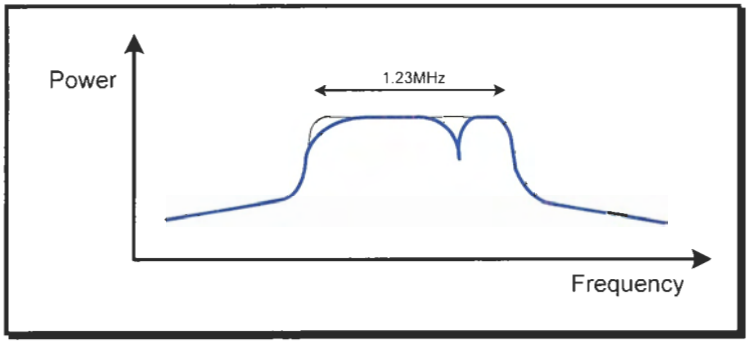

Figure 27 Example of Frequency Selective Fading

In rapid fades a narrowband signal would be completely lost by the receiver for a brief period. A wideband signal, however, will appear distorted in the frequency domain. In figure 27, the correct shape of the signal in the frequency is shown in black. The distorted signal is shown, in front, in colour.

In general, the coherence bandwidth is an indication of the frequency bandwidth which is expected to fade together. A signal which is wider than the coherence bandwidth will not suffer a fade of the entire signal at the same time. As a result the data contained in the signal is not lost but only degraded.

7.3 Fast Fading Resilience of a CDMA 1x Signal

A CDMA mobile station has at least four fingers to track the multipath signals and signals from other cell sites. When at least one of the multipath signals is greater than 0.814 μs the receiver places a second finger on that signal and demodulates it independently. It then performs maximal ratio combining on the output from all the fingers. Since multiple paths will not experience fades simultaneously, this has the effect of severely limiting effect of deep fades.

In the configuration tested, no soft handoff partners were provided. If they were, the mobile would be able to take advantage of macro spatial diversity in many weak signal cases to mitigate the effects for both fast and slow fading.

7.4 Averaging Performed by Mobile

Before reporting the signal through messaging or through a debug interface, mobile phone programmers have a propensity to perform averaging on the $(RSSI)_{dBm}$ and $(E_c/I_o)_{dB}$ measurements. This is a vender specific feature which may be performed to remove 'noise' from the signal so that a more stable measurement may be reported. The mobile receives an update every 20ms frame. Filtering 3 to 6 measurements results in a 60ms to 120ms averaging window. This is enough to remove many of the fast fading effects.

Part of this study was to see what data could be collected using a mobile phone rather than dedicated test equipment. This aspect may prove to be a critical limitation.

7.5 Expected Fading Performance

As a result of the frequency selective fading, the multiple fingers in the phone receiver, and possibly some averaging performed by the mobile a smocthed response is expected. A conceptual plot of these effects is shown in figure 28.

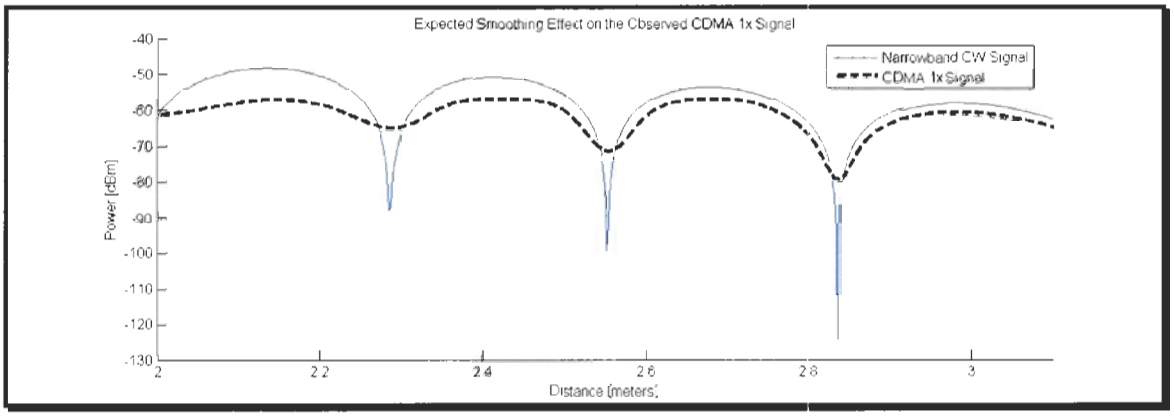

Figure 28 Expected Smoothing Effect on the Observed CDMA 1x Signal

As shown above the deep Rayleigh fades are eliminated. This is part of the design of a CDMA 1x system. The deep fades are quite detrimental and all digital systems must make efforts to account for them. Many narrowband systems rely primarily on baseband coding schemes to eliminate the effects of these fades. In addition to a wideband signal CDMA 1x uses baseband coding and fast power control.

7.6 Selection of the Fast Fading Component

After the work performed in section 6.2 the fast fading component is easily obtainable as shown in equation 13.

$$FastFadingComponent[dB] = CompositeFadingComponent - SlowFadingComponent \quad (13)$$

In practice the local means were subtracted from the composite fading signal for each data set, leaving just the fade fading component.

7.7 Statistical Distribution of the Fast Fading Component

Since land use varied throughout the measurement area, the data was divided into 9 smaller regions. The distribution of the fast fading component was analyzed in each region.

The CDF of the fast fading component in four representative regions are plotted below in figure 29. Compare these distributions to the reference distributions provided in figures 17, 18 and 19. With approximately 5000 data points plotted in regions 1, 7 and 8 it can be seen that the tails diverge only slightly when probabilities of about 25 in 5,000 are observed. Only 340 points are plotted in region 6 and almost no tail divergence is observed.

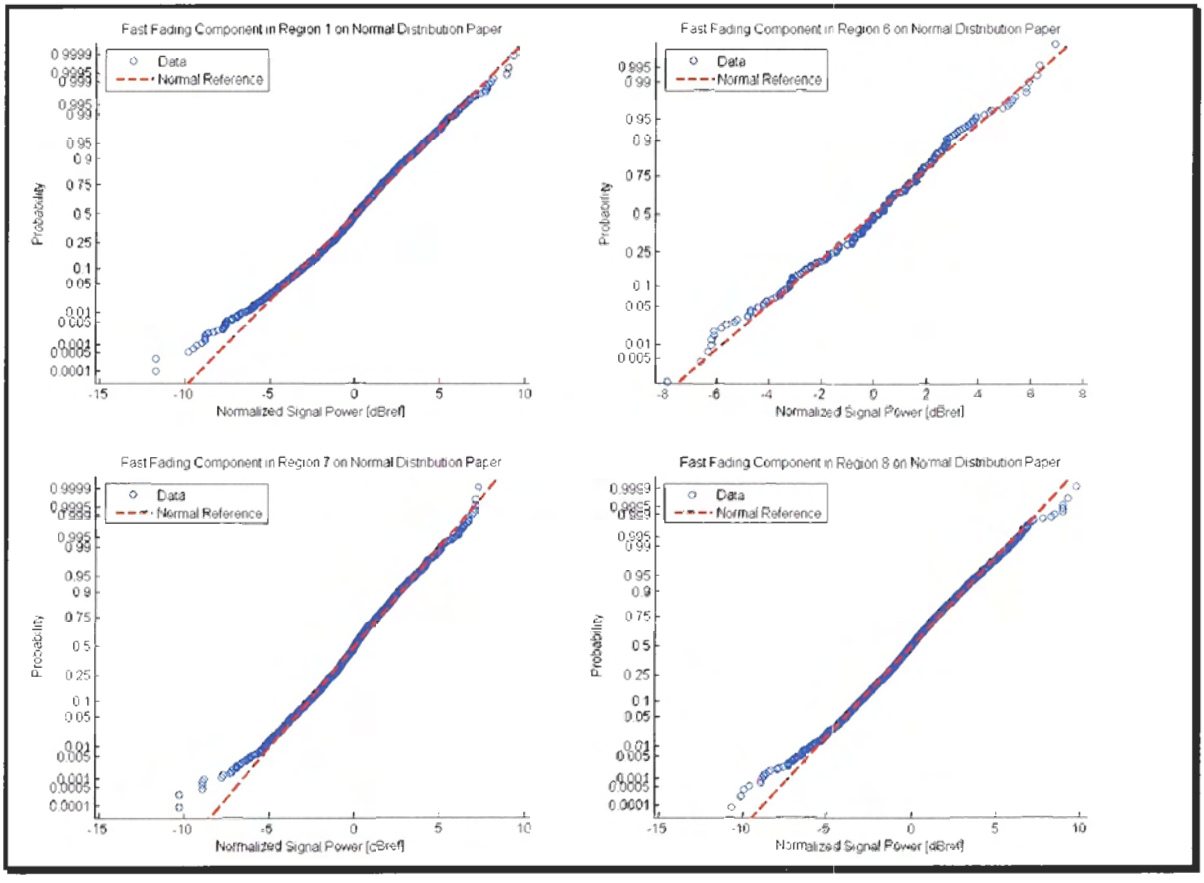

Figure 29 Distribution of Fast Fading Signal

The fast fading signal in all regions was examined and by comparison with the reference distributions each was found to be similar to a log-normal distribution. This would be surprising if a narrowband signal was being evaluated or if it the mitigating factors described in 7.1 through 7.5 were not present.

The standard deviation, σ, of the fast fading component in each region varied slightly as shown in figure 30. The variable, n, refers to how many measurements were recorded in each area.

1 σ=2.5dB n=4810	**2** σ=2.9dB n=8500	**3** σ=2.3dB n=250
4 σ=2.5dB n=10220	**5** σ=2.9dB n=14560	**6** σ=2.5dB n=340
7 σ=2.1dB n=5610	**8** σ=2.4dB n=6360	**9** n=1

Figure 30 Division of Measurement Area into Nine Smaller Regions

Similar results were seen when the measurement area was divided into 16 smaller regions rather than 9.

In essence then there is no fast fading component of this observed signal. Since temporal data was not recorded it is not possible to determine whether this is due to wideband effects, due to averaging of the received signal in the mobile or a combination of both.

Since there is no Rayleigh fading present, it does not matter during the slow fading analysis in section 6 whether the fast fading component is removed or if all the measured data is observed together.

8 AUTOCORRELATION ANALYSIS

8.1 1D Autocorrelation

Finally, the spatial autocorrelation of the smoothed slow fading component obtained in section 6.2 is analyzed. This distance based autocorrelation is a function of the clutter such as buildings, cars, infrastructure, foliage, and the like found in the measurement area. It can also be a measurement of undulations in the terrain. In this study, that is not the case since the terrain is almost perfectly flat.

8.1.1 Calculation of 1D Autocorrelation

First the mean path loss was removed from the data to produce the *SlowFadingComponent* of the signal which is a zero mean signal with units of dB and was analyzed in section 6. A selection of *SlowFadingComponent* data was chosen, as described below, which is represented by *x* in equation 14 below.

$$R_{xx}(m) = \begin{cases} \sum_{n=0}^{N-m-1} x_{n+m} x_n & m \geq 0 \\ R_{xx}(-m) & m < 0 \end{cases} \tag{14}$$

After applying equation 14 the result is normalized; providing the normalized spatial autocorrelation function, ρ. In previous studies [1], [2], [3], [5] the model provided in equation 15, has been found to represent ρ well.

$$\rho_{model} = \exp(-|d|/\Lambda) \tag{15}$$

The parameter Λ describes the decorrelation distance. The decorrelation distance is the distance beyond which the fading response is not expected to remain correlated. This distance is related to the size of the clutter in the measurement area.

8.1.2 Selection of Data Used for Analysis

Several long continuous strips of measurements were selected from the data base in order to evaluate autocorrelation. The criteria for selecting these strips were as follows:

- Less than 30 meters between data sets. There are 10 measurements per data set so this provides a measurement at least every 3 meters.
- Vehicle moving at least 50mm/second. In general the vehicle was moving much faster but this criterion was to make sure the vehicle wasn't stopped.
- A maximum of one data point removed, in previous steps, between each valid data set.

- A sequence of at least 90 sets of data, or 900 measurements.

These long strips were recorded contiguously but the vehicle was not necessarily travelling in a straight line.

In addition to the long continuous strips, three sets of straight north-south strips of data were created. This data was concatenated from a number of shorter data segments along the three major north-south routes in the measurement area. The strips are each about 1km long.

The location of the selected strips is shown below:

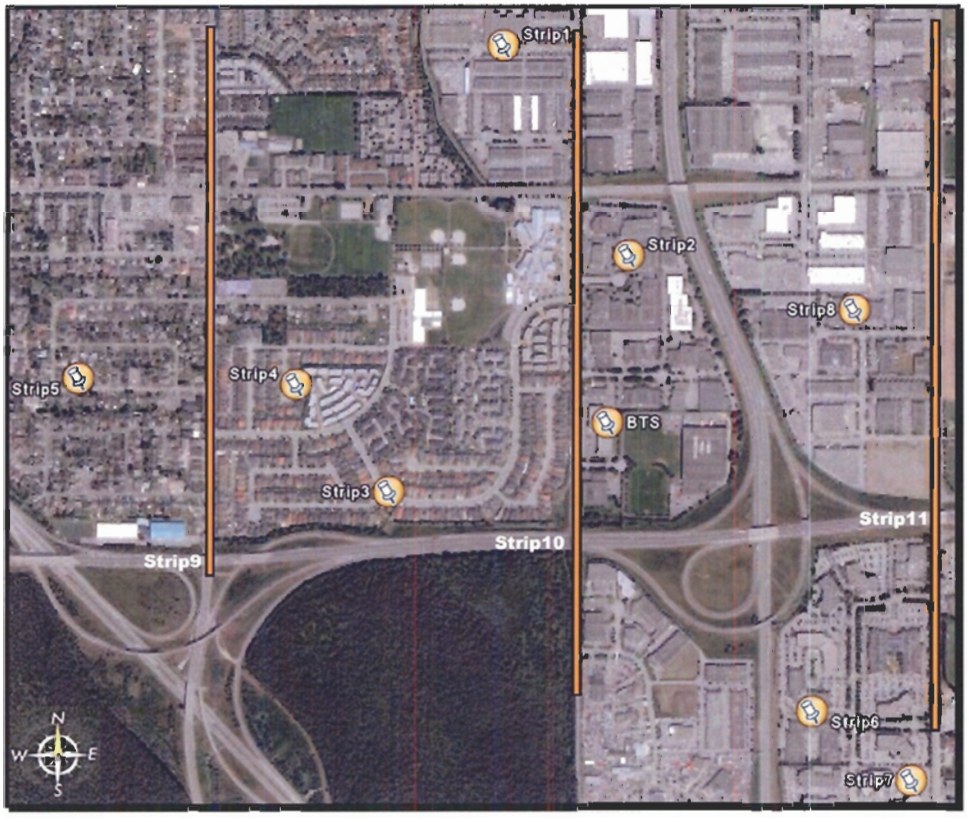

Figure 31 Location of Selected Strips of Measurement Data

To provide a sense of scale, consider that each parallel north-south strip is exactly ½ mile apart.

8.1.3 Resulting 1D Decorrelation Distances

Equation 16 is the natural log of equation 15.

$$\ln(\rho_{model}) = -|d| / \Lambda \qquad (16)$$

From this equation it can be seen the autocorrelation model is now linear. Further, the decorrelation distance is the point at which the trend line crosses the -1 mark on the y-axis.

The natural log of the measured autocorrelation function, ln(ρ), together with equation 16 are plotted for the four data strips selected from the residential areas shown in figure 31.

On the left the individual strips are shown in various colours. The heavy black line is the average of the autocorrelation plots. On the right the average is plotted along with an LMS fit of the model.

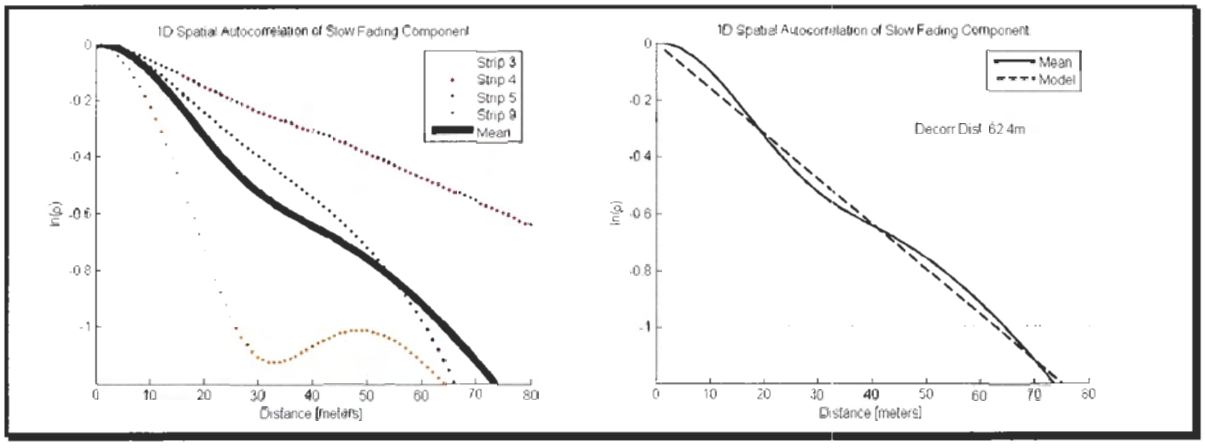

Figure 32 1D Spatial Autocorrelation of Slow Fading Component in Residential Area

In residential areas the average decorrelation distance is 62.4 meters.

In figure 33, the natural log of the measured autocorrelation function, ln(ρ), together with equation 16 is plotted for the five data strips selected from industrial areas.

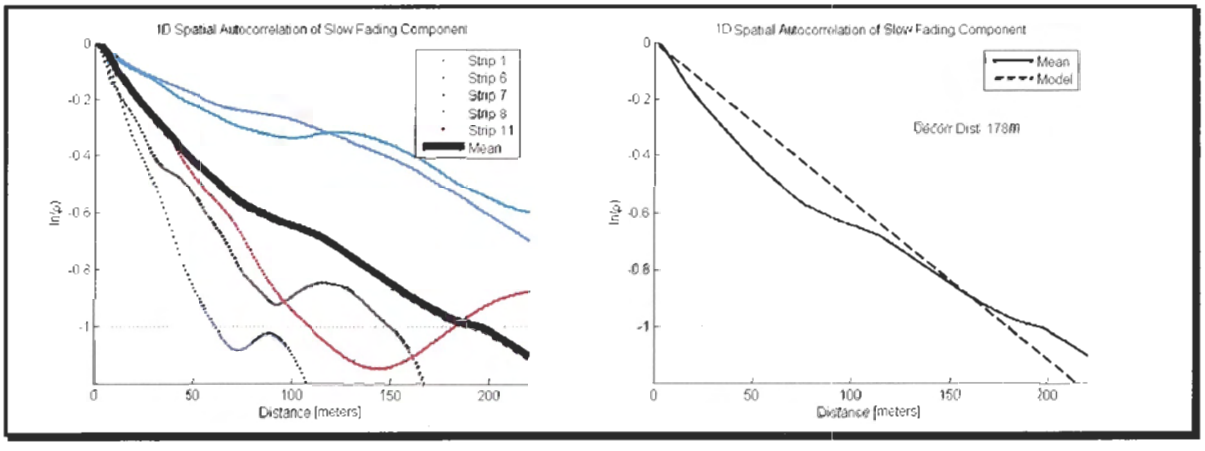

Figure 33 1D Spatial Autocorrelation of Slow Fading Component in Industrial Area

In industrial areas the average decorrelation distance is 178 meters.

While the decorrelation distance obviously varies between residential areas and industrial areas, there is still a fair amount of variation within each of the plots above. Some of that is due to a limitation in the amount of data analyzed but also some the variation appears to be due to the specific region from which the data was collected.

In table 8 the approximate building size perpendicular to the transmitter, as determined from Google Earth, is listed as well as the approximate decorrelation distance as determined from figures 32 and 33.

Source	Strip Number	Land Use Type	Building Size Perpendicular to the Transmitter	Decorrelation Distance
Long Strips	Strip 2	LOS	30 - 90m	20m
Straight Strips	Strip 10	LOS	50 - 70m	60m
Straight Strips	Strip 9	Residential	10 - 30m	30m
Long Strips	Strip 3	Residential	10 - 20m	50m
Long Strips	Strip 5	Residential	10 - 20m	60m
Long Strips	Strip 4	Residential	10 - 20m	110m
Long Strips	Strip 8	Industrial	40 - 80m	60m
Straight Strips	Strip 11	Industrial	50 - 150m	110m
Long Strips	Strip 7	Industrial	70 - 130m	150m
Long Strips	Strip 1	Industrial	70 - 100m	300m
Long Strips	Strip 6	Industrial	50 - 100m	400m

Table 8 Decorrelation Distance Compared to Typical Building Sizes

The land use marked line of sight (LOS) are areas close to the transmitter where a strong LOS component expected due to arrangement of the buildings. This stronger than average signal is also evident in figure 14. In the industrial and residential areas a definite relationship between the size of the buildings and the measured decorrelation distance is apparent. Refer to figure 34 below.

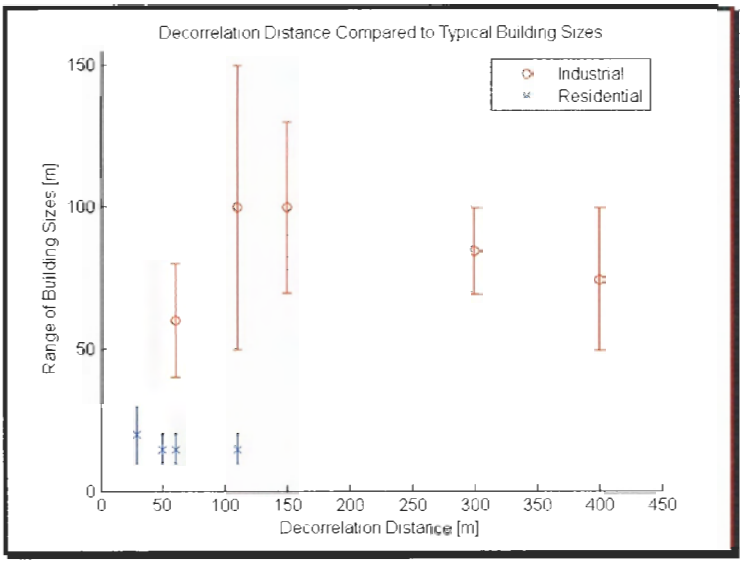

Figure 34 Decorrelation Distance Compared to Typical Building Sizes

Further analysis showed that the autocovariance of the slow fading component resulted in shorter decorrelation distances. However a relationship between decorrelation distance and building size similar to the one shown above remains when using the autocovariance rather than the autocorrelation.

8.1.4 Comparison with Results of Previous Researchers

Mawira [2] finds a bi-Markovian autocorrelation function with decorrelation distances of 100 meters and 1200 meters. The shorter distance is assumed to be to due to clutter such as buildings and the larger distance due to terrain.

Algans, Pedersen, and Mogensen [3] observe a decorrelation distance of 30 meters in suburban areas and a distance of 25 to 55 meters in typical urban areas.

Gudmundson [1] finds a decorrelation distance of 600 meters in suburban areas and a distance of 50 meters in urban areas.

Marsan [9] found a decorrelation distance of 44m, 1.6km from the transmitter, and a decorrelation distance of 112m, 4.8km from the transmitter.

Due to the high dependence on terrain and clutter the results vary quite a bit. The distances observed in this study fall within the range seen in other studies. More importantly they correlate well with the size of the clutter.

8.2 2D Autocorrelation

8.2.1 Interpolation and Regularization

To produce data that was regular enough to perform an autocorrelation function the measured points of the slow fading component were interpolated with a spline curve in a 2D sense. A grid of interpolated data points was produced with a regular spacing of 10

meters. For a graphical representation of the results of this interpolation refer back to figure 22.

Along the vehicle path no interpolation was required since more than enough data was collected. In empty spots, between roads for example, the interpolation typically added 3 to 10 data points between measurements. In the worse case areas up to 20 points were interpolated between each measured point.

Since this is the slow fading component, and as shown by the 1D results, the signal varies in the order of many tens of meters. Observation of the interpolated data showed that there were a sufficient number of measurements for the results to be justifiable in the vast majority of the area used for 2D analysis. Furthermore, the 2D results will also show that they correspond well with the 1D results.

8.2.2 Calculation of 2D Autocorrelation

As in the 1D case, the 2D autocorrelation is calculated based on the *SlowFadingComponent* of the signal. In this case a reasonably large 2D geographical area is selected, as shown in figures 12 and 22, rather than strips of data. The selected *SlowFadingComponent* is represented by *x* in equation 17 below.

$$C_{xx}(i,j) = \begin{cases} \sum_{m=0}^{Mx-1} \sum_{n=0}^{Nx-1} x_{m,n} x_{m+i,n+j} & i,j \geq 0 \\ C_{xx}(-i,-j) & i,j < 0 \end{cases} \qquad (17)$$

After applying equation 17 the result is normalized; providing the 2D normalized spatial autocorrelation function, ρ. The result is plotted below in figures 35 and 36. Note that, as with any autocorrelation plot, the data is symmetrical across the centre.

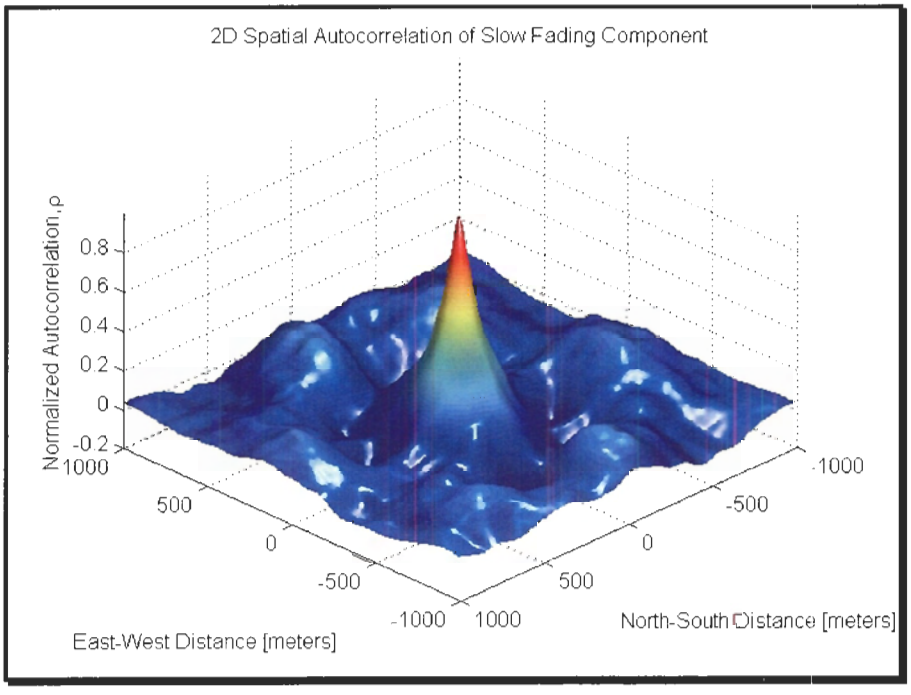

Figure 35 2D Spatial Autocorrelation of Slow Fading Component (3D Plot)

The above plot provides an average of the spatial autocorrelation throughout the selected region. This defines the rate at which the received power level is expected to change due to clutter in the environment. As discussed in section one of this paper, among other things, the 2D spatial autocorrelation will assist in the definition of the power control requirements which are specific to a particular sector or region.

The data which was used to produce this plot is the same data which may be collected by the BTS automatically during the course of operation. If the BTS was to produce such results for various regions within its coverage area it could adjust resources, such as the power control speed, to its required rate. It could also, for example, adjust the handoff parameters to a conservative setting or an aggressive setting based on the how rapidly the signal is expected to change.

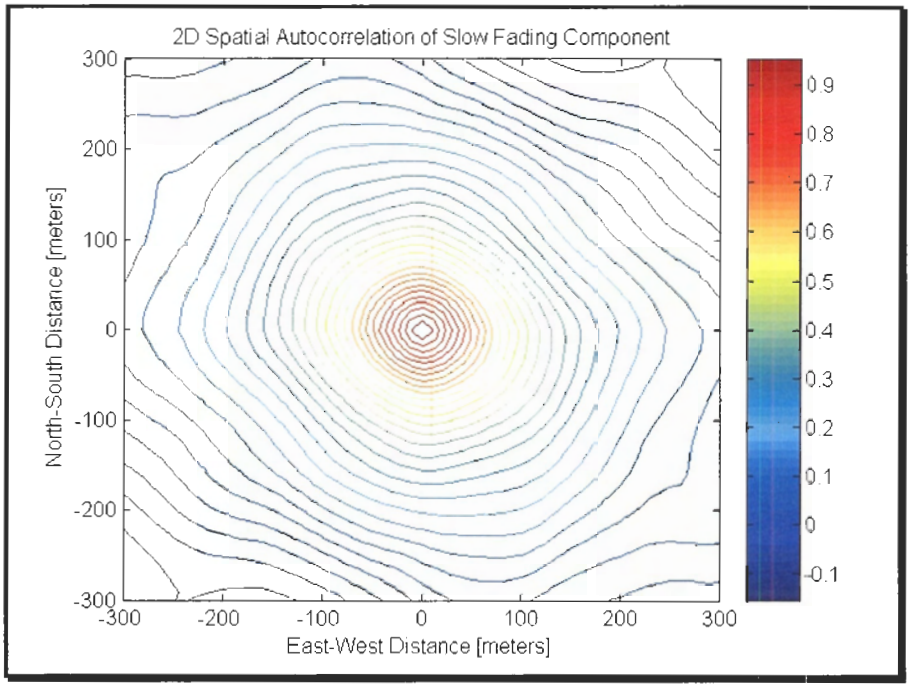

Figure 36 2D Spatial Autocorrelation of Slow Fading Component (2D Plot)

The figure above shows that the decorrelation distance depends very little on the direction of travel. In order to further analyze the 2D data, the plots above were divided into 36 slices representing 5 degrees each. Figure 37 again shows the natural log of the measured autocorrelation function, $\ln(\rho)$, together with equation 16; this time using slices of 2D data.

On the left the individual slices are shown in various colours. The heavy black line is the average of the autocorrelation slices. On the right the average is plotted along with an LMS fit of the model.

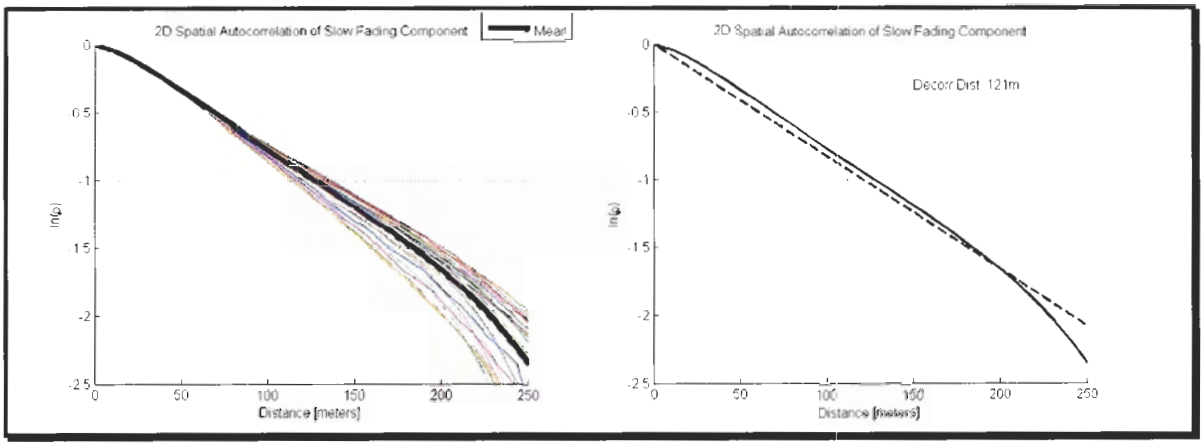

Figure 37 Slices of the 2D Spatial Autocorrelation of Slow Fading Component

Referring to the plot on the left of figure 37, it can be seen the slices of the figure 35 line up quite closely, which confirms that the 2D autocorrelation result is very uniform with respect to direction of travel.

From the plot on the right, the average 2D decorrelation distance is found to be 121 meters. This happens to be the average of residential and the industrial 1D decorrelation distances which were previously found to be 62.4 meters and 178 meters respectively. This is expected since the 2D autocorrelation incorporates data collected from all regions.

Since much more data was analyze here than in the 1D cases, the response is much more predictable and stays consistent with the model down to about $\ln(\rho)= -2$.

9 SUMMARY AND CONCLUSIONS

It has been shown that a significant amount detail can be determined about the fading channel using data collected from a handset. Much of the information required to tune network parameters and optimize algorithms has been produced in this report.

It was found that correcting for the antenna pattern was a prerequisite to understanding the any of the data collected. Once this was done, the mean path loss was evaluated. The Cost231 model was found to fit the data well and a mean path loss exponent of 3.61 was observed.

The slow fading component was separated and found to have a log-normal distribution with a standard deviation of 6.0 dB. The fast fading component was expected to be Rayleigh but due to wideband effects, and due to averaging performed by the mobile, it was observed to be log-normal with a standard deviation of between 2 and 3dB. Consequently the composite fading component, the fast and slow fading components combined, had a log-normal distribution with a standard deviation of 6.6dB.

Since fast fading data could not be obtained with sufficient detail and since there is currently no way to retrieve the finger offset information from the phone over the air some aspects of the channel could not be analyzed. Specifically, since delay spread and the actual fast fading distribution are unknown it is not possible to perform any temporal analysis.

The 1D autocorrelation of the slow fading component of the signal was calculated and found to have an average decorrelation distance of 62.4 meters in residential areas and an average decorrelation distance of 178 meters in industrial areas. The 2D autocorrelation of the signal was also calculated, providing an extension to the results of previous researchers. The 2D autocorrelation was found to be directionally uniform and the 2D decorrelation distance was found to be 121 meters. This represents an average for several different land uses in the measurement area and is very close to the mean of the 1D results.

Of more interest than the absolute decorrelation distance is the change in the decorrelation distance for different land use types. A direct relationship between typical building sizes and the decorrelation distance was found to be present. However, more study is required to better understand this relationship.

This study has shown that the concept of collecting valuable data using just a user terminal is feasible. The next steps are to implement data collection into the BTS software which will ultimately allow the users will supply system performance information. A large database with over 50,000 good measurements is available and can used to evaluate data collected from the BTS once the appropriate software has been implemented.

APPENDIX

Below is the output of the executed Matlab scripts. Upon request the measurement database, and Matlab source code can be made available. The data gathering software, written in C, can not be made available but direction can be provided on how to produce such software.

```
>> runme

%%%%%%%%%%%%%%%%%%%%%%%%%%%%%%%%%%%%
       Gather Reference Data
%%%%%%%%%%%%%%%%%%%%%%%%%%%%%%%%%%%%

FILENAME =
Reference10.csv
Reading Full Data Sets:
        1980
No Satellite Lock:
     0
Not Registered or No Pilot:
     0
Create meanRssi, meanEcio...
Calculating Distance from the Center...

Radius Stats...
Mean: 1.9223m
Max: 5.1699m
Min: 0.029668m
Spread: 5.1402m
Variance: 0.98471m
Sigma: 0.99233m
90th Percentile: 3.3209m

Altitude...
Mean: 86.5752m
Max: 101.7m
Min: 71.7m
Spread: 30m
Variance: 40.9075m
Sigma: 6.3959m
90th Percentile: 8.5248m

Number Sats...
Min: 4

Mean RSSI...
Mean: -65.798dB
Max: -64dB
Min: -84.5dB
Spread: 20.5dB
Variance: 1.3583dB
```

```
Sigma: 1.1655dB
90th Percentile: 0.79798dB

RSSI...
Mean: -65.798dB
Max: -63dB
Min: -92dB
Spread: 29dB
Variance: 1.6378dB
Sigma: 1.2797dB
90th Percentile: 0.79798dB

Mean Ec/Io...
Mean: -5.6223dB
Max: -4dB
Min: -15.8dB
Spread: 11.8dB
Variance: 0.4622dB
Sigma: 0.67985dB
90th Percentile: 0.62232dB

Ec/Io...
Mean: -5.6223dB
Max: -4dB
Min: -21dB
Spread: 17dB
Variance: 0.65739dB
Sigma: 0.8108dB
90th Percentile: 0.62232dB

Plotting Error vs. Measured Radius...
Plotting Location of 2D Data...

%%%%%%%%%%%%%%%%%%%%%%%%%%%%%%%%%%
    Plot Reference Distributions
%%%%%%%%%%%%%%%%%%%%%%%%%%%%%%%%%%

Plot PDF...
Plot Fit on Normal Paper...
Plot PDF...
Plot Fit on Normal Paper...
Plot PDF...
Plot Fit on Normal Paper...

%%%%%%%%%%%%%%%%%%%%%%%%%
       Gather Data
%%%%%%%%%%%%%%%%%%%%%%%%%

FILENAME =
ABCDE10.csv
Reading Full Data Sets:
        7738
No Satellite Lock:
     4
Not Registered or No Pilot:
        2351
```

```
Purging Bad Rows...
Duplicates Found During Purge:
     2
Speed Information Calculated...
Finding Peak...
Calculating Distance from the Peak...
Producing X and Y...
Exceeding Minimum/Maximum Distance from the Peak:
     0
Exceeding Max Altitude:
   168
Purging Bad Rows Again...
Plotting Speed Histogram...
Mean Speed: 25.1km/hr
Plotting Location of 2D Data...

%%%%%%%%%%%%%%%%%%%%%%%%%
  Mean PL / Slow Fading
%%%%%%%%%%%%%%%%%%%%%%%%%

Plotting Antenna Pattern...
Plotting Pilot Strength Including Antenna Gain...
Calculate and Plot Mean Square Error Trend Line...
Pathloss Exponent: 3.61
Equiv 1m Pathloss: -2.17dB
Plotting Pilot Signal Strength Corrected for Antenna Gain...
Plot PDF...
Plot Fit on Normal Paper...
Mean: -6.0989e-014
Sigma: 6.5812
Plot PDF...
Plot Fit on Normal Paper...
Mean: -6.298e-014
Sigma: 6.0279

%%%%%%%%%%%%%%%%%%%%%%%%%
      Fast Fading
%%%%%%%%%%%%%%%%%%%%%%%%%

Create Fast Fading Data...
Region: 1
Plot PDF...
Plot Fit on Normal Paper...
Mean: 2.3e-016 Sigma: 2.4595 Length: 4810
~~~~~~~~~~~~~~~~~~~~~~~~~~~~~~~~~~~~~~~~~~~~~~~~~~~~
Region: 2
Plot PDF...
Plot Fit on Normal Paper...
Mean: -1.5e-016 Sigma: 2.8998 Length: 8500
~~~~~~~~~~~~~~~~~~~~~~~~~~~~~~~~~~~~~~~~~~~~~~~~~~~~
Region: 3
Plot PDF...
Plot Fit on Normal Paper...
Mean: 1.1e-016 Sigma: 2.2825 Length: 250
~~~~~~~~~~~~~~~~~~~~~~~~~~~~~~~~~~~~~~~~~~~~~~~~~~~~
Region: 4
```

```
Plot PDF...
Plot Fit on Normal Paper...
Mean: -1.1e-016 Sigma: 2.5048 Length: 10220
~~~~~~~~~~~~~~~~~~~~~~~~~~~~~~~~~~~~~~~~~~~~~~~~
Region: 5
Plot PDF...
Plot Fit on Normal Paper...
Mean: 1.3e-016 Sigma: 2.926 Length: 14560
~~~~~~~~~~~~~~~~~~~~~~~~~~~~~~~~~~~~~~~~~~~~~~~~
Region: 6
Plot PDF...
Plot Fit on Normal Paper...
Mean: -5e-016 Sigma: 2.5071 Length: 340
~~~~~~~~~~~~~~~~~~~~~~~~~~~~~~~~~~~~~~~~~~~~~~~~
Region: 7
Plot PDF...
Plot Fit on Normal Paper...
Mean: 3.3e-016 Sigma: 2.1238 Length: 5610
~~~~~~~~~~~~~~~~~~~~~~~~~~~~~~~~~~~~~~~~~~~~~~~~
Region: 8
Plot PDF...
Plot Fit on Normal Paper...
Mean: 0 Sigma: 2.3679 Length: 6360
~~~~~~~~~~~~~~~~~~~~~~~~~~~~~~~~~~~~~~~~~~~~~~~~

%%%%%%%%%%%%%%%%%%%%%%%%
2D Linear AutoCorrelation
%%%%%%%%%%%%%%%%%%%%%%%%

Residential...
Create Strips of Nearly Consecutive Data Points...
Show Where the Strips Are...
Create N-S Strips of Data...
Show Where the Strips Are...
Merge Long and NS Strips...
Interpolate Data...
Calculate and Show Spatial Autocorrelation...
Strip: 3 Negl approx: -0.994 Decorr Distance: 45
Strip: 4 Negl approx: -1     Decorr Distance: 110
Strip: 5 Negl approx: -1.01  Decorr Distance: 62
Strip: 9 Negl approx: -1.01  Decorr Distance: 27
Produce Trendline for Mean Spatial Autocorrelation...
Industrial...
Create Strips of Nearly Consecutive Data Points...
Show Where the Strips Are...
Create N-S Strips of Data...
Show Where the Strips Are...
Merge Long and NS Strips...
Interpolate Data...
Calculate and Show Spatial Autocorrelation...
Strip: 1 Negl approx:  -1      Decorr Distance: 300
Strip: 6 Negl approx:  -1      Decorr Distance: 400
Strip: 7 Negl approx:  -0.994  Decorr Distance: 150
Strip: 8 Negl approx:  -0.996  Decorr Distance: 62
Strip: 11 Negl approx: -0.994  Decorr Distance: 109
Produce Trendline for Mean Spatial Autocorrelation...
```

```
%%%%%%%%%%%%%%%%%%%%%%%%%
      3D Analysis
%%%%%%%%%%%%%%%%%%%%%%%%%

FILENAME =
ABCDE10.csv
Reading Full Data Sets:
        7738
No Satellite Lock:
     4
Not Registered or No Pilot:
        2351
Purging Bad Rows...
Duplicates Found During Purge:
     2
Speed Information Calculated...
Finding Peak...
Calculating Distance from the Peak...
Producing X and Y...
Exceeding Minimum/Maximum Distance from the Peak:
        1210
Exceeding Max Altitude:
   168
Purging Bad Rows Again...
Plotting Location of 2D Data...
Plot 3D Altitude...
Plot 3D Altitude...complete
Plot 3D Pilot Power...
Plot 3D Pilot Power...complete
Plot 3D Normalized Pilot Power...
Plot 3D Normalized Pilot Power...complete

%%%%%%%%%%%%%%%%%%%%%%%%%
   3D AutoCorrelation
%%%%%%%%%%%%%%%%%%%%%%%%%

Plot 3D AutoCorrelation...
Plot 3D AutoCorrelation...complete
Plot Slices of Autocorrelation...
Plot Selected Slices of Autocorrelation...
Plot All Slices of Autocorrelation...
Plot Mean of Slices of Autocorrelation with Trendline...
```

REFERENCE LIST

[1] M. Gudmundson, "Correlation model for shadow fading in mobile radio systems," *IEE Electron. Lett.*, vol. 27, pp. 2145-2126, Oct. 1992.

[2] A. Mawira, "Models for the spatial correlation functions of the log-normal component of the variability of VHF/UHF field strength in urban environment," *Proc. Personal, Indoor and Mobile Radio Communications* (PIMRC'92), 1992, pp. 436-440.

[3] A. Algans, K. Pedersen and P. Mogensen, "Experimental Analysis of the Joint Statistical Properties of Azimuth Spread, Delay Spread, and Shadow Fading," *IEEE Journal on Selected Areas in Communications*, vol. 20, pp. 523-531, Apr. 2002.

[4] M. LeCours et al., "Statistical Modeling of the Received Signal Envelope in a Mobile Radio Channel," *IEEE Transactions on Vehicular Technology*, vol. 37, pp. 204-212, Nov. 1988.

[5] S. R. Saunders, *Antennas and Propagation for Wireless Communication Systems*. West Sussex: Wiley, 1999.

[6] D.M. Black and D.O. Reudink, "Some characteristics of mobile radio propagation at 836 MHz in the Philadelphia area," *IEEE Trans. Veh. Tech.*, 21 (2), 45-51, 1972.

[7] Third Generation Partnership Project 2. *Recommended Minimum Performance Standards for cdma2000 Spread Spectrum Base Stations*, 3GPP2 C.S0010-A, 2001. Available at HTTP: www.3gpp2.org

[8] Y. Okumura, et al., "Field strength and its variability in VHF and UHF land mobile radio service," *Rev. Electr. Commun. Lab.*, 16, 825-73, 1968.

[9] M.J. Marsan, G.C. Hess, and S.S. Gilbert, "Shadowing variability in an urban land mobile environment at 900MHz," *Electronics Letters*, 26 (10), 646-48, 1990.

[10] The City of Richmond, "Zoning District Schedule". Available at HTTP: www.richmond.ca

[11] J. Griffiths, *Radio Wave Propagation and Antennas*. Prentice-Hall, 1987.

[12] COST231 Final Report, *Digital Mobile Radio: COST 231 View on The Evolution Towards 3rd Generation Systems*. Brussels: Commission of the European Communities and COST Telecommunications, 1999.

[13] R. Vaughan and J.B. Andersen, *Channels, Propagation and Antennas for Mobile Communications*. Institution of Electrical Engineers, 2003.

[14] W.C. Jakes, Ed., *Microwave Mobile Communications*. New York: IEEE Press, 1994.

[15] W.C. Y. Lee, "Estimate of local average power of a mobile radio signal", *IEEE Trans. Veh. Technol.*, vol. VT-34, no. 1, pp. 22-27, Feb. 1985.

[16] N. Bajj, *Chirp for Mobile Radio Channel Characterisation*. Ph.D. Thesis, University of Manchester, 1997.

[17] J.J. Egli, "Radio Propagation above 40MC over irregular terrain", *Proc. IRE*, 1383-91, 1957.

[18] W.C.Y. Lee, *Mobile Communications Engineering*. New York: McGraw-Hill, 1982.

[19] W.C.Y. Lee, *Mobile Design Fundamentals*. New York: John Wiley, 1993.

[20] M.F. Ibrahim and J.D. Parsons, "Signal strength prediction in built-up areas", *Proc. IEE*, 130F (5), 377-84, 1983.

[21] K. Allesbrook and J.D. Parsons, "Mobile radio propagation in British cities at frequencies in the VHF and UHF bands," *IEEE Trans. Veh. Tech.,* 26(4), 95-102, 1977.

[22] J. Walfisch, and H.L. Bertoni, "A theoretical model of UHF propagation in urban environments," IEEE Trans. Ant. Prop., 36(12), 1788-96, 1988.